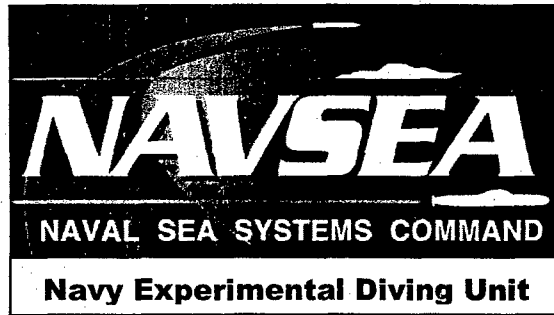


**Navy Experimental Diving Unit
321 Bullfinch Rd.
Panama City, FL 32407-7015**

**TA 01-07
NEDU TR 04-42
December 2004**

PROBABILITY OF DECOMPRESSION SICKNESS IN NO-STOP AIR DIVING



20060210 055

Authors: H. D. Van Liew, Ph.D.
E. T. Flynn, M.D.

**Distribution Statement A:
Approved for public release;
distribution is unlimited.**

UNCLASSIFIED

SECURITY CLASSIFICATION OF THIS PAGE

REPORT DOCUMENTATION PAGE			
1a. REPORT SECURITY CLASSIFICATION Unclassified		1b. RESTRICTIVE MARKINGS	
2a. SECURITY CLASSIFICATION AUTHORITY		3. DISTRIBUTION/AVAILABILITY OF REPORT DISTRIBUTION STATEMENT A: Approved for public release; distribution is unlimited.	
2b. DECLASSIFICATION/DOWNGRADING AUTHORITY			
4. PERFORMING ORGANIZATION REPORT NUMBER(S) NEDU Technical Report No. 04-42		5. MONITORING ORGANIZATION REPORT NUMBER(S)	
6a. NAME OF PERFORMING ORGANIZATION Navy Experimental Diving Unit	6b. OFFICE SYMBOL (If Applicable)	7a. NAME OF MONITORING ORGANIZATION	
6c. ADDRESS (City, State, and ZIP Code) 321 Bullfinch Road, Panama City, FL 32407-7015		7b. ADDRESS (City, State, and Zip Code)	
8a. NAME OF FUNDING SPONSORING ORGANIZATION Naval Sea Systems Command	8b. OFFICE SYMBOL (If Applicable) OOC	9. PROCUREMENT INSTRUMENT IDENTIFICATION NUMBER	
8c. ADDRESS (City, State, and ZIP Code) 1333 Isaac Hull Ave, S.E. Washington Navy Yard, D.C. 20376-1073		10. SOURCE OF FUNDING NUMBERS Naval Sea Systems Command	
		PROGRAM ELEMENT NO. 0603713N	PROJECT NO. S0099
		TASK NO. 01A	WORK UNIT ACCESSION NO. 99-04 & 01-07
11. TITLE (Include Security Classification) (U) Probability of Decompression Sickness in No-Stop Air Diving			
12. PERSONAL AUTHOR(S) Hugh D. Van Liew, Ph.D.; Edward T. Flynn, M.D.			
13a. TYPE OF REPORT Technical Report	13b. TIME COVERED FROM 1997 TO 2002	14. DATE OF REPORT December 2004	15. PAGE COUNT 45
16. SUPPLEMENTARY NOTATION			
17. COSATI CODES		18. SUBJECT TERMS (Continue on reverse if necessary and identify by block number)	
FIELD	GROUP	SUB-GROUP	Bends, Decompression sickness, Diver safety, No-Stop dives, No-D dives, Probabilistic models, Undersea medicine
19. ABSTRACT. We produce statistics-based (probabilistic) and intuition-based (deterministic) models using dive-outcome data from the U.S. Navy Decompression Database to gain an understanding of the no-stop diving instructions used by the U.S. Navy and various other navies. The models allow estimation of probability of decompression sickness (DCS) for various bottom times for air no-stop diving. Our calibration dataset contains 2,037 experimental no-stop dives with 104 cases of decompression sickness (DCS) and covers a large range of depths and bottom times; unfortunately the data are not well distributed with regard to depth, bottom time, and DCS incidence. Our probabilistic model shows good agreement between predictions and observations. We augment the same calibration dataset with a few dives that have short decompression stops to produce the deterministic model. According to our models, probability of decompression sickness (P_{DCS}) is 2% or less for current U.S. Navy schedules for most no-stop air dives and near 1% for no-stop schedules of the navies of Great Britain, Canada, and France. Our probabilistic model serves well to provide P_{DCS} estimates and time limits that are similar to those in current use by navies for most of the range of standard air diving and for subsaturation diving, but it fails for short, deep dives in two ways: it fails to avoid observed DCS cases in our calibration dataset, and it indicates that bottom time can be longer than bottom times in current use by the navies we examined. For short, deep dives, we recommend depth/bottom-time combinations yielded by our deterministic model.			
20. DISTRIBUTION/AVAILABILITY OF ABSTRACT		21. ABSTRACT SECURITY CLASSIFICATION	
<input type="checkbox"/> UNCLASSIFIED/UNLIMITED	<input checked="" type="checkbox"/> SAME AS RPT.	<input type="checkbox"/> DTIC USERS	Unclassified
22a. NAME OF RESPONSIBLE INDIVIDUAL NEDU Librarian		22b. TELEPHONE (Include Area Code) 850-230-3100	22c. OFFICE SYMBOL

THIS PAGE INTENTIONALLY LEFT BLANK

FOREWORD

This work was supported in part by the Deep Submergence Biomedical Development Program, Naval Sea Systems Command, Task Numbers 63713N S0099 01A 99-04 and 63713N S0099 01A 01-07. The opinions and assertions contained herein are the personal views of the authors and are not to be construed as official or as reflecting the views of the Navy Experimental Diving Unit or the U.S. Navy.

THIS PAGE INTENTIONALLY LEFT BLANK

CONTENTS

	<u>Page No.</u>
DD Form 1473	i
Foreword	ii
Contents	iii
Figures and Tables.....	iv
Introduction	1
Methods	3
No-Stop Spreadsheet	3
Distributions of the Variables	5
Probabilistic No-Stop Models	8
Deterministic No-Stop Model	10
Results	13
Probabilistic Model	13
Deterministic Model	19
Discussion	23
No-Stop Limits of Other Navies	23
Pitfalls in Probabilistic Modeling	25
Tables of DCS Probability	27
Conclusions	32
References	34
Appendix: Details of DCS cases	A-1 – A-4

THIS PAGE INTENTIONALLY LEFT BLANK

FIGURES

Figure 1. A dive profile	2
Figure 2. Distributions of variables	7
Figure 3. Dive-outcome graphs	11
Figure 4. Dive-outcomes and P_{DCS} isopleths	15
Figure 5. DCS incidences in subdivisions of the data.....	16
Figure 6. Observations vs. predictions, no-stop dives	18
Figure 7. P_{DCS} for shallow dives.....	19
Figure 8. Observations vs. predictions, subsaturation dives.....	20
Figure 9. Deterministic model.....	21
Figure 10. VVal-18 and StandAir Models	22
Figure 11. Comparisons for various navies	24
Figure 12. P_{DCS} vs. depth.....	25
Figure 13. Dose-response curves	31

TABLES

Table 1. Source files for the calibration dataset.....	6
Table 2. Special DCS cases.....	13
Table 3. Parameters for the Probabilistic No-Stop Model.....	14
Table 4. Limits by our models and by other navies	23
Table 5. Time limits by our models and by the USN table	28
Table 6. P_{DCS} for various profiles	30
Table 7. Time limits for subsaturation no-stop dives	32
Table 8. P_{DCS} for subsaturation and shallow dives.....	33

PAGE INTENTIONALLY LEFT BLANK

INTRODUCTION

Most military, commercial, and recreational dives are "no-stop dives," known also as "no-decompression dives." Divers following the depth/bottom-time instructions for no-stop diving can ascend directly to the surface with a low probability of contracting decompression sickness (DCS). In contrast, divers who remain at a certain depth longer than the maximal time prescribed by no-stop instructions are obliged to ascend to the surface by using "stops" of prescribed times at prescribed depths. In 1993 the U.S. Navy changed the ascent rate from 60 to 30 feet of seawater/min for the U.S. Navy Standard Air Decompression Table¹ (USN57) and in 1999 added no-stop limits for dives at 25 and 30 feet of seawater, gauge (fswg; 1 fsw = 3.063 kPa; 33.08 fswg = 2 atmospheres absolute).

The USN57 decompression table and tables used by other navies are "deterministic"; they carry an underlying assumption that dives are either safe or unsafe, an assumption implying that there is a threshold for developing DCS. Deterministic models are generated by an intuitive method in which recorded outcomes of test dives and impressions from operational dives are used informally. A more modern alternative is to use statistical methods to develop "probabilistic" models,^{2,3} which assume that there is a graded response to decompression stress, so that even ostensibly safe dives carry small but finite risks.

Probabilistic models are generated by fitting dive-outcome data to equations or algorithms, thus tying decompression instructions to objective facts about dive outcomes. Probabilistic models allow a probability statement to be assigned to any dive profile, so distinctions can be made between particular DCS cases that occur in relatively safe dives and those that occur in hazardous dives. When speaking of a probabilistic model, we mean the probability equation or algorithm used to fit the "calibration data" plus the values of the parameters found by the fit. Our calibration data — information about whether divers were stricken with DCS after experimental dives — are from the U.S. Navy Decompression Database.^{4,5}

In 1982 Leitch and Barnard⁶ reviewed no-stop instructions used by navies of the United States, Great Britain, and France and the test dives that had been instrumental in generating the three sets of instructions.⁷⁻⁹ Since that time there have been minor adjustments to the tables.¹⁰⁻¹² It is reasonable to assume that the no-stop instructions adopted by these various navies are acceptably safe; if this were not so, the navies would have replaced their tables. However, it is not clear what the probabilities of DCS are.

Our long-term goal is to develop a set of nitrogen-based decompression tables that correct safety and capability deficiencies of current U.S. Navy tables. To that end, we developed a probabilistic model for standard air diving¹³ that provides prescriptions for dives with decompression stops as well as for no-stop dives. Objectives of this report are to review existing no-stop dive instructions in the light of probabilistic and deterministic models that we generate and to estimate probability of contracting DCS

after no-stop dives with various bottom times. The results offer informed choices for divers who may be obliged to remain at depth longer than stipulated by current no-stop instructions.

Bottom times lasting a day or longer are considered "saturation" dives; we assume that body tissues come close to equilibrium with the inert gas of the breathing mixture in 24 hours. We deal with saturation dives in another study.¹⁴ No-stop dives shallower than 40 fswg with bottom times between 4 hr and one day (240 to 1,440 min) are used in ship husbandry; they are in the transition between standard dives and saturation dives. A recent probabilistic model¹⁵ which we will call "NMRI '93" led to a recommendation to shorten the bottom times for these no-stop subsaturation dives. Such shortening would cause a major decrease in the efficiency of U.S. Navy operations. Clarification of the risks of subsaturation diving could also be important in management of rescuers and personnel being rescued from disabled submarines. Submariners may be at depth long enough to become saturated, whereas rescuers, who may be exposed to pressure for shorter times than the submariners, are in a subsaturation status.

The U.S. Navy Decompression Database

The box at the top of Figure 1 illustrates a heading that summarizes the actual dive profile for a test dive as it is compiled in the U.S. Navy Decompression Database.^{4,5} The top line gives the dive depth in fswg; the bottom time in minutes; and time, in

minutes, for ascent to the surface called "total decompression time" (TDT). The TDT is the sum of times at decompression stops and travel time. Next (between the last comma and the end of the line) is a coded comment about the profile and its relation to other profiles in the same series.

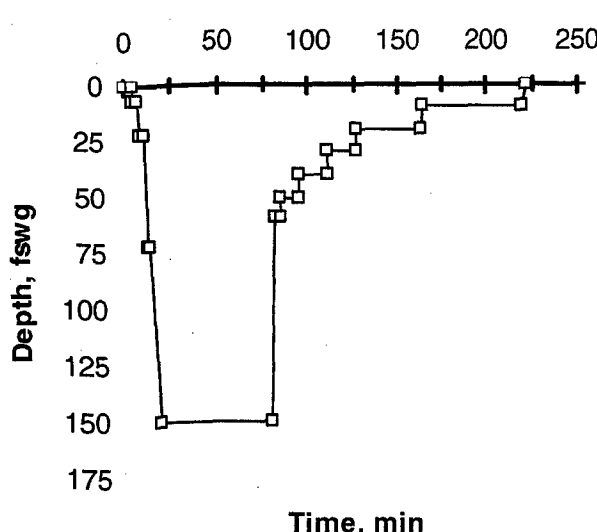


Figure 1. Illustration of an entry in the U.S. Navy Decompression Database. The box shows a sample heading for a dive profile from file EDU1180S. The plot of depth below sea level vs. time is from the body of the tabulation, which is not shown here.

In the second line of the heading, "1.000" signifies the gas breathed before the dive (1.000 is the code for air), and the next "1" indicates the number of person-dives included in this particular profile. The "1.0" indicates that this diver suffered DCS; the value here would be zero if no DCS had resulted and "0.5" if the DCS were considered a "marginal" case, one having signs or symptoms that are diagnosed as DCS but not severe enough to require treatment. The "252.0" in the second line of the

heading is T1, the last time since the start of the dive that the diver was surely free of signs or symptoms of DCS, and the "312.0" is T2, the first time that signs or symptoms of DCS were noted. Units of T1 and T2 are minutes.

In a database entry, the heading is followed by a body of information about the dive profile. The times and depths plotted in Figure 1 are from the body. The dive is to 150 fswg, with bottom time of 73.2 min and TDT of 143.8 min, including six decompression stops. The observation period extends beyond the graph to 1,662 min. If the diver breathes a gas mixture other than air during the dive, codes in the body of the profile indicate the mixture and the times and depths at which the breathing of the non-air mixture commenced and stopped.

METHODS

NO-STOP SPREADSHEET

From the U.S. Navy Decompression Database^{4,5} we prepared a "parent" Microsoft Excel spreadsheet of single-level, nonrepetitive dives for which the breathing gases are various nitrogen-oxygen mixtures; air is the breathing gas for 72% of the total person-dives. In the Database a separate report describes the 23 source files, each of which contains a series of entries that provide information about one to 86 persons who followed a particular dive profile.

To prepare the spreadsheet, we carefully studied the details of the time and depth profiles of each entry, using the heading of the entry as a guide (see Figure 1). We deleted profiles having more than one distinct bottom depth or an indistinct series of bottom depths. When the recorded information in a profile indicated that the heading was inaccurate or that there was a small deviation from a square-wave exposure to depth, we made appropriate corrections so that the corrected depth, bottom time, and TDT pattern corresponded approximately to square-wave behavior. Delays at the beginning and end of the dives necessitated by far the most corrections. Data files DC4D, DC4W, and EDU885A needed the most corrections. We made corrections in 311 profiles representing 1051 person-dives; there were 150 person-dive corrections for depth (average absolute change = 1.59 fswg), 732 for bottom time (average absolute change = 3.74 min), and 474 for TDT depth (average absolute change = 2.49 min).

- 1) We took bottom time to be the difference between the time when the divers left a depth of 3 fswg or shallower and the time when the divers left the bottom depth.
- 2) All profiles of EDU885A needed correction for lags at 7 fswg at the beginning of the dives, with an average correction of $-2.54 \text{ min} \pm 1.34 \text{ min}$ standard deviation (SD).
- 3) We took the TDT to be the difference between the time when the divers left the bottom depth and the time when they reached a depth of 3 fswg or shallower.

- 4) We adjusted for irregularities in the depth so that the area under a graph of depth vs. bottom time is approximately equal to the area under an uncorrected graph:
- When the summary heading did not account for a delay near the final bottom depth, we made the bottom depth less.
 - When the summary heading did not account for a slow descent to depth, we shortened bottom time and/or decreased bottom depth.
 - When the summary heading did not account for small variations in bottom depth, we took average depth.

To use dives in which the breathing gas is a nitrogen mixture with an oxygen fraction different from that of air, we calculate an "equivalent air depth" (*EAD*, with units of fswg):

$$EAD = \left(\frac{1 - FO_2}{0.79} \right) \cdot (D + 33) - 33 \quad (1)$$

In Equation 1, FO_2 is inspired fraction of oxygen, 0.79 is the fraction of N_2 in air, D is actual depth of the dive in fswg, and 33 is the atmospheric pressure at the surface expressed in fswa (feet of seawater, absolute). In the remainder of this report, the word "depth" refers either to the actual depth (if divers breathed air) or to the *EAD* (if divers breathed a nitrogen mixture with an oxygen percentage different from that of air). When a fixed partial pressure of O_2 was breathed, we calculate the FO_2 for Equation 1 as $FO_2 = PO_2 / (1 + D/33)$, where PO_2 is the fixed partial pressure in atmospheres absolute.

We assume that a probabilistic model intended to generate instructions for a particular type of dive will be best if it is calibrated with data from that type of dive. Accordingly, we prepared a second spreadsheet comprised only of no-stop dives, the "No-Stop spreadsheet." To do so, we calculated two items for each entry in the parent spreadsheet: (1) an "expected" ascent time (*Exp* — divide the bottom depth by the ascent rate that the U.S. Navy currently prescribes, 30 fsw/min), and (2) the ratio of actual documented time for ascent to the expected time for ascent (*TDT/Exp*). Many dives used an ascent rate of 60 fsw/min, so many no-stop entries have *TDT/Exp* near 0.5. Our definition of no-stop dives is based on rate of ascent, not on absence of stops in the profile; we exclude dives that have long ascents, even though they have no definite decompression stops. Also, a few accepted dives have short stops or short delays during ascent. Some *TDT/Exp* ratios for no-stop dives are above 1.0 because of idiosyncratic delays in ascent or because some of the chambers used for long-duration dives cannot be exhausted at a rate of 30 fsw/min. In the No-Stop spreadsheet we exclude dives having the *TDT/Exp* ratio below 0.46 and above 1.5, with two exceptions: (1) we extend the *TDT/Exp* ratio to 1.6 for a few shallow dives (between 37 and 41 fswg) with long bottom times (between 302 and 720 min), and (2) we are lenient with saturation dives, as described in the paragraph that follows. Note that we would exclude the sample dive shown in Figure 1 because the diver spent more than two hours at decompression stops and thus has a high *TDT/Exp* ratio.

The No-Stop spreadsheet for calibration of our no-stop models includes 246 person-dives, 12% of the total, with bottom times of 1,440 min (1 day) or longer. We include these no-stop saturation dives in the spreadsheet to compensate for a lack of subsaturation dives. Thus, to make recommendations about subsaturation dives with bottom times between a half day and a full day, we are obliged to interpolate between saturation dives and standard air dives. The No-Stop spreadsheet contains 181 saturation dives with air breathing (18 DCS cases, average depth = 24.4 fswg) and 65 person-dives for which the breathing gas is a fixed partial pressure of 0.4 atmospheres (atm) of oxygen in nitrogen (4 DCS cases, average depth 23.3 fswg). Only 20% of the saturation dives meet our criterion for TDT/Exp of 1.5 or below. We accept saturation dives that have TDT/Exp up to 21 (TDT up to 14 min, average TDT/Exp = 15.1, average depth = 21.2 fswg). We assume that these longer ascents do not introduce bias because tissue susceptible to DCS for saturation dives releases excess gas slowly.

Table 1 provides a summary of the source files; files containing saturation dives appear in rows 16 through 23, inclusive. The totals at the bottom show 104 DCS cases among the 2,037 person-dives (see Appendix). After rereading the original documentation for file EDU159A,¹⁶ we revised the information in it; the revised file is EDU159AVL. Row 22 in Table 1 is for one no-stop saturation dive to 38 fswg, an air-breathing dive that resulted in DCS (unpublished observation on file at NEDU, Panama City, FL — “Outline of Results Incident to Dives (Compressed Air Exposures) Performed in the Pressure Chamber of the Experimental Diving Unit, Dec-May 1939–1940”). The right-hand column of Table 1 gives information on the TDT/Exp ratio. The incidence columns (DCS cases/100 person-dives) are for observed incidence (% Obs) and predicted incidence (% Pred). The Cases Pred and % Pred columns refer to results from the statistical fitting of data for the probabilistic P-No-Stop Model; they will be examined in the **RESULTS** section.

Some source files are specialized; for example, profiles in row 17 record saturation dives having small ranges of depths and times, whereas row 3 includes a large range of depths and times. Some files are for mild and some for hazardous exposures: row 1 records only one DCS case in 289 person-dives, whereas row 6 records 26 cases in 141 person-dives. In the source files, 123 person-dives in the No-Stop dataset are designated as “marginal”; for our purposes, we assigned these to be no-DCS cases. Marginal outcomes have the same bottom times and depths as DCS cases, with only a few exceptions.

DISTRIBUTIONS OF THE VARIABLES

Figure 2 shows distributions of pertinent variables in the No-Stop spreadsheet. In Figure 2A, number of person-dives decreases as depth increases, and the inset shows that incidence of DCS is unevenly distributed through the depth categories, with the second and fourth having incidences that are 50% or 25% as high as those in the other two. In Figure 2B, numbers of person-dives are unevenly spread across the range of bottom times, with about 40% of the person-dives lasting less than one hour. There are no data for the 120 to 179 min category; the star in the inset is for zero DCS cases

TABLE 1. SOURCE FILES FOR THE NO-STOP SPREADSHEET

Depth, bottom time, and ratio columns show ranges of values within the file

Source file	Entries	Depth	Bottom time	Person -dives	Cases Obs	Cases Pred	% Obs	% Pred	TDT/Exp Ratio
1 DC4D	86	50 – 262	5 – 75	289	1	1.8	0.3	0.6	0.5 – 1.4
2 DC4W	41	57 – 265	5 – 60	69	3	.8	4.3	1.2	0.5 – 1.0
3 EDU1351NL	43	44 – 189	5 – 205	143	2	3.8	1.4	2.7	1.2
4 EDU159AVL	5	34 – 36	720	11	5	1.7	45.5	15.5	1.0
5 EDU557	21	37 – 297	5 – 270	104	0	1.0	0.0	1.0	0.5 – 1.5
6 EDU849LT2	74	100 – 150	27 – 60	141	26	28.8	18.4	20.4	1.2
7 EDU849S2	35	33 – 40	720	60	13	13.8	21.7	23.0	1.2
8 EDU885A	16	60 – 190	12 – 67	112	4	2.9	3.6	2.6	0.8 – 1.2
9 NMR8697	229	30 – 111	30 – 240	477	11	10.6	2.3	2.2	0.6 – 0.8
10 NMR97NOD	9	40 – 41	199	103	3	1.9	2.9	1.8	1.5
11 NMRNSW	43	39 – 62	82 – 364	86	5	3.5	5.8	4.1	0.5 – 1.1
12 NSM6HR	16	32 – 40	359 – 360	47	3	2.0	6.4	4.3	0.5 – 1.6
13 PASA	3	102	35 – 38	5	1	0.3	20.0	6.0	0.7 – 1.0
14 RNPL52BL	7	50 – 150	11 – 90	87	0	0.9	0.0	1.0	0.5
15 RNPLX50	16	31 – 41	240 – 720	57	5	9.0	8.8	15.8	1.0
								!	
16 ASATARE	20	21 – 25	2,862 – 2,882	65	4	3.3	6.2	5.1	1.6 – 7.9
17 ASATDC	15	26 – 33	1,440 – 1454	23	8	3.7	34.8	16.1	0.9 – 3.4
18 ASATFR85	3	23 – 30	2,160	13	0	1.1	0.0	8.5	2.0 – 2.6
19 ASATNMR	34	20 – 24	4,320 – 6,181	50	1	2.0	2.0	4.0	0.5 – 21.0
20 ASATTNSM	13	26 – 30	2,880	34	4	5.0	11.8	14.7	1.4 – 1.5
21 EDUAS45	5	33	1,440 – 2,160	12	2	4.2	16.7	35.0	1.8
22 NEDU corresp.	1	38	1,440	1	1	0.6	100.0	60.0	1.0
23 NMR9209	15	20 – 23	4,284 – 4,400	48	2	1.6	4.2	3.3	9.6 – 18.0
Totals	750			2,037	104	104 ± 26.5*			

* 95% confidence interval of the prediction

among zero dives. The inset shows that DCS incidence is highest in the right-hand category, which includes all the saturation dives and subsaturation dives at 720 min. We define subsaturation dives as dives between 240 and 1,440 min; there are no person-dives at all between 721 min and 1,440 min, half of the possible range. The only subsaturation dives in the dataset are 261 person-dives with 7 DCS cases at bottom times of 240 min to 719 min and 118 person-dives with 23 DCS cases at 720

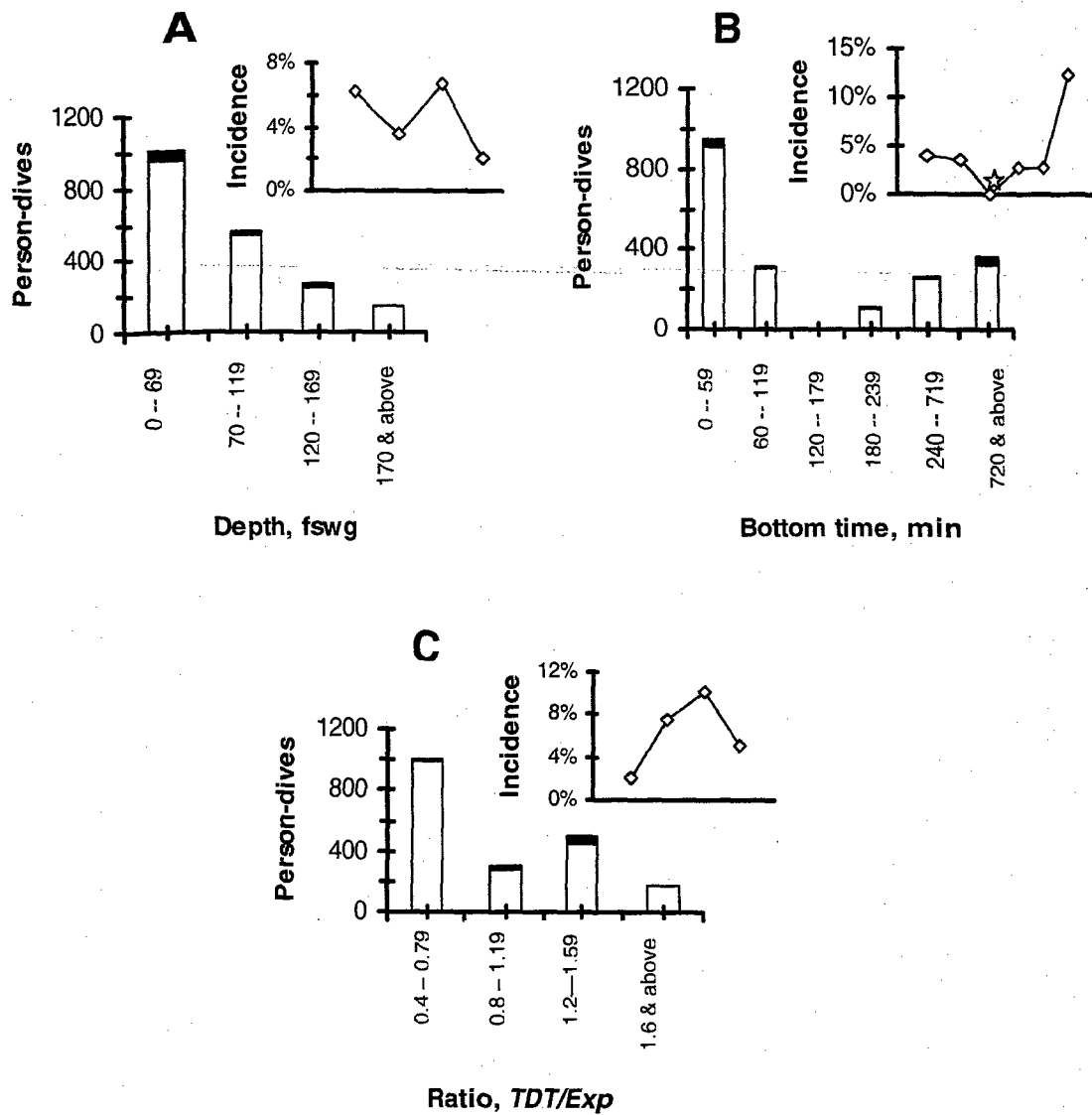


Figure 2. Frequency distributions of variables in the No-Stop spreadsheet. Height of columns shows total numbers of person-dives; height of black sections at the top shows numbers of DCS cases. Insets show incidence of DCS in the categories of the main graphs. A: depth (including air-equivalent depth for person-dives in which non-air N₂-O₂ mixtures are breathed). B: bottom time. C: ratio of observed TDT to expected TDT.

min. The saturation dives are weighted toward high DCS incidence (8.9% versus 5.1% for the entire dataset), have a wide range of bottom times (1,440 to 6,181 min), and have a small range of depths or air-equivalent depths (from 20 to 38 fswg). Figure 2C shows uneven distribution of the *TDT/Exp* ratio; the category with *TDT/Exp* ratio below 0.8 includes the most person-dives, and the inset shows its DCS incidence is the lowest.

A practical probabilistic model gives instructions for achieving a low incidence of DCS, so it is desirable to have many low-incidence dives in the dive-outcome information used to calibrate the model. According to the probabilistic P-No-Stop Model we will

describe, estimated probability of decompression sickness (P_{DCS}) is less than 3% for 62% of the total number of person-dives. The distribution of person-dives in this low- P_{DCS} subset of the data is approximately the same as that in Figure 2. This low-incidence range includes 17 DCS cases, most of which are for shallow dives with rapid ascent.

We use the No-Stop spreadsheet to develop both probabilistic and deterministic models.

Major models:

- P-No-Stop Model — probabilistic, based on the entire No-Stop spreadsheet.
- D-No-Stop Model — deterministic, based on the entire No-Stop spreadsheet plus a few dives with short times at decompression stops.

Minor models:

- Sat-Only Model — probabilistic, based on the saturation dives in the No-Stop spreadsheet and used only for the Likelihood Ratio statistical test.
- No-Sat Model — probabilistic, based on the entire No-Stop spreadsheet minus saturation dives and used only for the Likelihood Ratio statistical test.

PROBABILISTIC NO-STOP MODELS

Equation 2 characterizes probability in the logistic regression paradigm:

$$P_{DCS} = \frac{1}{1+e^{(-LOGIT)}} \quad (2)$$

Logistic regression is often used with a simple $LOGIT$ function:

$$LOGIT = b_0 + b_1 \cdot X_1 + b_2 \cdot X_2 + b_3 \cdot X_3 + \dots \quad (3)$$

The X_i are variables in the data, and b_i are parameters to be estimated by the statistical method. The *NONLIN* module of SYSTAT,¹⁷ a commercial statistical program, allows us to use a complex formula for the variable corresponding to X_1 in Equation 3. After exploring other possibilities, we decided upon a particular $LOGIT$ function:

$$LOGIT = a + b \cdot D \cdot [(1 - e^{(-cT)}) + d \cdot (1 - e^{(-fT)})] \quad (4)$$

Variables in Equation 4 are dive depth in fswg (D) and bottom time in min (T). Five parameters (a , b , c , d , and f) are estimated by the statistical process.

In Equation 4 the exponential form for the two terms containing T allows for the effect of bottom time to stabilize after long times, a result consistent with the idea that P_{DCS} does not depend on bottom time after tissues are saturated with gas. For a given P_{DCS} , the product of depth and bracketed time functions is equal to a constant over the entire range of no-stop diving. Hempleman¹⁸ suggested a similar proposition: that the product of depth and the square root of time is the operative function.

To understand Equation 4, consider the conventional ideas that the body is composed of distinct compartments or tissues that have various absorption rates for inert gases and that the underlying cause of DCS is supersaturation of inert gas in a "critical" compartment during ascent from depth. For deep dives, compartments having short halftimes are critical, so bottom times are short. Compartments with longer halftimes are critical in shallower dives, and compartments with the longest halftimes are critical in saturation dives. Equation 4 accounts for uptake of inert gas in a hypothetical pair of compartments. According to the parameters to be discussed, one compartment has halftime of 21.5 minutes; the halftime of the second compartment, 420 minutes, is somewhat longer than the 360-minute halftime often used in modeling of altitude decompression.¹⁹ The parameter estimation process indicates that, for a given degree of equilibration, the DCS risk associated with the slow compartment is 2.76 times greater than the risk associated with the fast compartment.

The *NONLIN* module of SYSTAT provides an option, the *LOSS*, for characterizing an error statement that differs from the conventional least-squared-errors statement used in statistics. Equation 5 is the *LOSS* statement we use; it is in terms of a single dive-outcome entry:

$$LOSS = -DIVES \cdot [DCS \cdot \ln(ESTIMATE) + noDCS \cdot \ln(1 - ESTIMATE)] \quad (5)$$

In Equation 5, *DIVES* is the number of person-dives in the group test that makes up the dive-outcome entry, *DCS* indicates whether subjects in the group contracted DCS, *ln* signifies natural logarithms, *ESTIMATE* is the estimated P_{DCS} , and *noDCS* indicates that no subjects in the group had DCS. The *DCS* variable is either a one or a zero, because divers who dived together but did not contract DCS are listed together in the same profile (*DCS* = 0, *DIVERS* = number of divers), but divers with DCS are listed separately (*DCS* = 1, *Divers* = 1). The *LOSS* function is the sum of *LOSS* statements given by Equation 5 over the entire calibration dataset.

To begin estimating parameters, the SYSTAT program uses Equations 2 and 4 with tentative, user-generated starting values of the parameters to calculate an initial P_{DCS} for the first dive-outcome data point. Then Equation 5 calculates the *LOSS* value from that P_{DCS} . The procedure is repeated for all data points, and the *LOSS* is summed over all points. The summed *LOSS* is recalculated iteratively to find a minimum *LOSS* by a

quasi-Newton iteration process that uses the first and second derivatives of the *LOSS* function to find new tentative parameter values. The iterations continue until differences between successive tentative parameter estimates reach a predetermined small value. The minimized positive *LOSS* is the same as a maximized negative log likelihood (*LL*) for maximum likelihood estimation of parameters. In addition to parameter estimation, the *NONLIN* module computes asymptotic standard errors (*ASE*) and the asymptotic correlation matrix of parameters by estimating the Hessian (second derivative) matrix.

Three kinds of 95% confidence intervals are of interest. (1) From the limited-sized samples of person-dives, we use the binomial theorem to calculate intervals for the "true" incidences of DCS in the entire population. (2) The intervals for estimated parameters are given by the *NONLIN* module's output. (3) From results of the statistical analysis (parameters, *ASEs*, and correlation matrix), we use the equations described by Ku²⁰ to calculate intervals for the estimated *Pdcs*; with the Ku equations, the *Pdcs* and confidence intervals can be tabulated for the *D-T* pair for each entry in the calibration dataset or for entries in a set of decompression instructions.

Chi-square tests assess whether differences between observed DCS cases in the calibration data and predicted cases from the model are greater than expected from chance:

$$\chi^2 = \sum (Co - Cp)^2/Cp \quad (6)$$

where *Co* is cases observed in a subset of the data and *Cp* is cases predicted in the same subset. Small values of the calculated χ^2 value indicate that the model is a good fit to the calibration data.

DETERMINISTIC NO-STOP MODEL

Figure 3 illustrates our method for generating a deterministic model and also shows an alternative to Figure 2 for viewing the distribution of depths and times in the calibration dataset. In the panels of Figure 3, no-stop dives fall in a hyperbolic shape on a plot of bottom time versus depth; divers can stay at a shallow depth for a long time, at a medium depth for an intermediate time, and deep for a short time. Triangles indicate DCS cases that occurred after a dive to the depth/bottom-time pair indicated by the coordinates. For DCS cases in divers who breathed a gas mixture with oxygen different from the fraction of O₂ in air (0.21), the triangles are accompanied by special symbols (see the caption to Figure 3).

Two bull's-eye symbols between 150 and 200 fswg in Figure 3, almost superimposed on each other, correspond to 3 DCS cases associated with dives having decompression stops. These bull's-eye dives are in the parent spreadsheet but not in the No-Stop calibration data. Clinical descriptions of them in the source files are limited.^{4,5} We include them for our deterministic model on the assumption that if DCS occurs with dives having short times at decompression stops, DCS is also likely with no-stop dives having the same depths and bottom times.

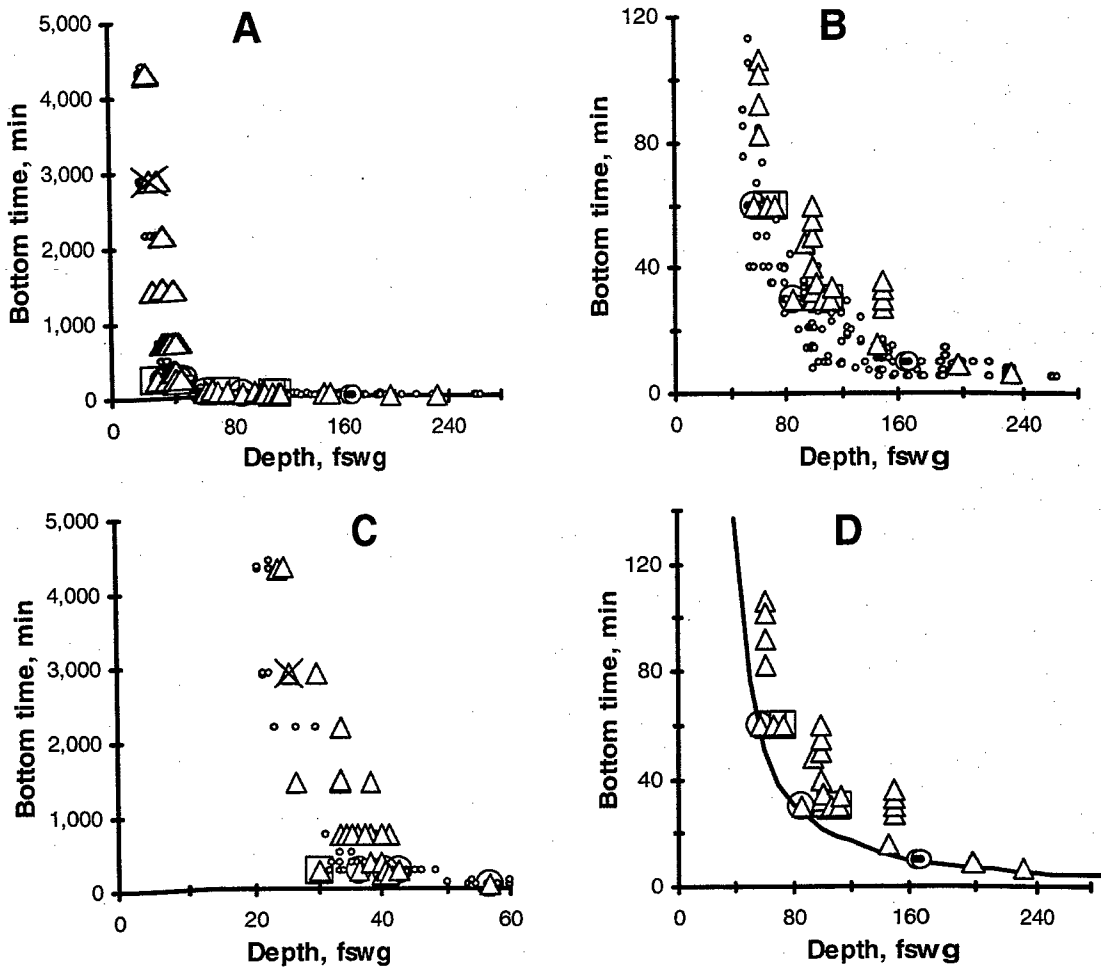


Figure 3. Plots of the dive-outcome data. Triangles = DCS cases in one subject or, rarely, two subjects. Small circles = no DCS in a number of subjects (subjects/circle = 1 to 86, average = 3). Triangles with large circles = DCS cases in which the subject breathed a mixture with FO_2 below 0.21. Triangles with large squares = DCS cases in which the subject breathed a mixture with FO_2 above 0.21. Triangles with large X = four DCS cases in which the subject breathed a fixed PO_2 . Bull's-eye shapes = three selected DCS cases in which the profile included short decompression stops. A: all the data; most small circles are obscured by triangles. B: short bottom-time range. C: shallow-depth range. D: illustration of our method of generating deterministic no-stop instructions by fashioning a curve below or to the left of DCS cases seen in panel B.

dives having short times at decompression stops, DCS is also likely with no-stop dives having the same depths and bottom times.

Consider any particular depth in Figure 3: theoretically, a diver who remains at that depth for a short time should be free of DCS, so the symbol for the dive on the Figure 3 axes would be a small circle. A diver who remains at the depth too long may contract DCS; if so, the symbol would be a triangle. Thus, circles should predominate at the lower edge of the hyperbolic shape, and triangles should predominate at the upper edge. Such a configuration is visible in Figure 3B, where a region containing only small circles is below another region where there are triangles.

Since our models are concerned only with no-stop dives, our deterministic model can be very simple. We need only to differentiate between profiles that provoked DCS and those that did not. In contrast, deterministic models for dives that entail decompression stops during ascent must track tissue gases in order to introduce a decompression stop whenever a compartment is at a dangerous level of supersaturation. The principle of our approach is to separate DCS-free dives from those that cause DCS on a depth versus bottom-time plot. We fashion a curve, by eye, to the left of all the DCS cases that have been observed in the experimental dive trials. The guiding rules for drawing the curve are that it should avoid the triangles and should curve smoothly. The method is illustrated in Figure 3D, which shows the DCS cases from Figure 3B. We call the deterministic model defined by the curve in Figure 3D the "D-No-Stop Model": it is below or to the left of the bull's-eye symbols and all the DCS cases (triangles) in the No-Stop dataset. Drawing this curve is clearly a subjective process that is imprecise because of the gaps between the data points. We arbitrarily limit the D-No-Stop Model to depths of 40 fswg and deeper; bottom times are between zero and 137 min.

Although a deterministic model is, by definition, not concerned with P_{DCS} , we can use a probabilistic point of view to speculate about our D-No-Stop Model. It takes 148 dives with no DCS cases to say with 95% confidence that incidence is below 2% (one-tailed binomial distribution), so some of the symbols for DCS-free dives (small circles) in Figure 3 may actually be for dives that have a fairly high probability for causing DCS. The maximum number of dives per circle on the graphs is only 86, so we cannot be confident that P_{DCS} is less than 2% for any of the small circles. A few of the triangles can be associated with P_{DCS} less than 2%, but most probably correspond to higher P_{DCS} . In the face of such uncertainties, we are assuming that any triangle indicates that the probability of DCS is above an acceptable level when we locate a curve to the left of the triangles.

In all of the data used here, seven DCS cases are noticeably to the left of the trend of the triangle DCS case symbols:

- The bull's-eye symbols at the lower right of Figure 3D stand for three DCS cases.
- Two triangles inside large circles are at equivalent depths of 57 and 85 fswg for divers breathing FO_2 lower than 0.21; one of these stands for two DCS cases [numbers (2), (3), and (4) in Table 2].
- An additional DCS case is off scale on Figure 3D; it is for a diver breathing FO_2 higher than 0.21 [number (1) in Table 2, a triangle inside a large square that is visible in Figures 3A and 3C, equivalent depth = 30 fswg, bottom time = 240 min].

Table 2 gives details of the four DCS cases from the seven in which divers breathed non-air mixtures. All cases in Table 2 are from the same source file, and the

TABLE 2. NON-AIR DCS CASES WHICH ARE TO THE LEFT OF THE TREND OF TRIANGLES IN FIGURE 3

<u>Source file</u>	Actual depth, fswg	Equiv depth, fswg	Bottom time, min	TDT, min	Ratio <i>TDT/Exp</i>	T2, min	FO ₂
(1) NMR8697	50	30	240	1.2	0.8	601	0.4
(2) NMR8697	46	57	60	1.1	0.8	166	0.1
(3) NMR8697	46	57	60	1.1	0.7	781	0.1
(4) NMR8697	71	85	30	1.5	0.6	272	0.1

Equiv depth = equivalent air depth, calculated by Equation 1.

TDT = total decompression time; equals travel time for no-stop diving.

TDT/Exp Ratio = observed TDT divided by TDT expected with an ascent rate of 30 fsw/min.

T2 = first time the subject has symptoms of DCS, timed from the start of the dive.

FO₂ = fraction of O₂ in gas breathed at depth.

subjects switched from the fixed fraction of O₂ to air at 30 fswg during ascent. We suspect that either these particular dives are aberrant or that breathing a non-air mixture carries a greater DCS risk than breathing air does. In either case, the non-air dives may represent a different population from air dives.

Six of the seven DCS cases that are to the left of the trend determine the position of the D-No-Stop Model curve in Figure 3D; they are cases identified by bull's-eyes and circled triangles in the first two bullets above. Non-air dives represent half of the dives that determine the depth/bottom-time combinations of the D-No-Stop Model; non-air dives also affect our probabilistic models, but their impact on the statistical fit is diluted because the bulk of the calibration dives are air dives.

RESULTS

PROBABILISTIC MODEL

Table 3 presents parameters for the probabilistic "P-No-Stop Model," that are estimated using the No-Stop spreadsheet. The LL value is much better than the LL for the null model, in which *Pdcs* = *inc*, the DCS incidence for the calibration dataset. The parameters are more than six times greater than their standard errors in all cases. The correlation matrix indicates that some of the parameters are correlated with each other, especially parameters *c* and *d*. An equation having three exponential terms and no weighting parameter for any of the terms gives the same LL as the P-No-Stop Model, but the time constants for two of the exponential terms are the same, indicating to us that Equation 4, with two exponential terms and weighting of the second by parameter *d*, is preferable to having three exponential terms. An equation with three exponential terms in which two were weighted did not improve the LL.

TABLE 3. PARAMETERS FOR THE P-NO-STOP MODEL

Equation 4: $LOGIT = a + b \cdot D \cdot [(1 - e^{(-c \cdot T)}) + d \cdot (1 - e^{(-f \cdot T)})]$

Model = No-Stop, Equation 4, $LL = -323.41$ Null model, $LL = -410.68$, $inc = 5.1\%$

Parameter	Estimate	ASE*	Param/ASE	95% Confidence Interval
a	-8.837279	0.382609	-23.10	-9.59 – -8.09
b	0.068630	0.008662	7.92	0.0516 – 0.0856
c	0.032453	0.005125	6.33	0.0224 – 0.0425
d	2.760433	0.379541	7.27	2.015 – 3.506
f	0.001651	0.000182	9.06	0.001293 – 0.002008

Correlation matrix

	a	b	c	d	f
a	1.000000				
b	-0.571482	1.000000			
c	0.127428	-0.852794	1.000000		
d	0.175982	-0.879394	0.944642	1.000000	
f	0.081734	-0.597798	0.58453	0.495313	1.000000

* ASE = asymptotic standard errors

We used Equation 4 to calibrate two additional models: the “Sat-Only Model,” calibrated with the saturation data alone, giving LL of -56.44, and a “No-Sat Model” based on 1,741 person-dives that remained in the No-Stop spreadsheet after all the saturation data were removed, giving LL of -265.19. We performed a Likelihood Ratio (LR) test^{21–23} with these two minor probabilistic models plus the P-No-Stop Model to learn whether it is advisable to combine data from saturation and nonsaturation no-stop dives. The LR test determines whether two datasets, when combined, are described as well as they are by two separate evaluations. Our test compares the sum of the LL values of the evaluations using saturation data alone and nonsaturation data alone with the LL value of the evaluation using the combined data:

$$LR = 2 [(LL_{\text{Sat-Only}} + LL_{\text{No-Sat}}) - LL_{\text{No-Stop}}] \quad (7)$$

The LR calculated by Equation 7 is compared with the value of the chi-square distribution with $k + j - p$ degrees of freedom, where k and j are the numbers of parameters in the Sat-Only and No-Sat evaluations, respectively, and p is the number of parameters in the No-Stop evaluation. The evaluation of Equation 7 is $LR = 2 \{ [(-56.44) + (-265.19)] - (-323.41) \} = 3.56$. The chi-square value for $2 + 5 - 5 = 2$ degrees of freedom and 95% confidence is 5.99. The calculated value of LR of 3.56 is less than 5.99, the chi-square value, an indication that the datasets can be combined.

Predictions versus observations: P-No-Stop Model

The equation for the least-squares trend line for a plot of the Cases Pred (Y) versus the Cases Obs (X) columns of Table 1 is $Y = 1.0425X - 0.1791$, with square of the correlation coefficient (R^2) of 0.91. The slope of the line is nearly 1.0 and the intercept nearly zero, indications that the P-No-Stop Model is a reasonably good predictor of the DCS cases in the source files.

Figure 4 displays P_{DCS} isopleths calculated from the parameters of the P-No-Stop Model along with dive-outcome data in Figure 3. The trace for 2% P_{DCS} in panel A has several triangles below or to the left of it, but the trace for 1% P_{DCS} in panel B avoids most triangles; the exception is for deep dives at the right of panel B.

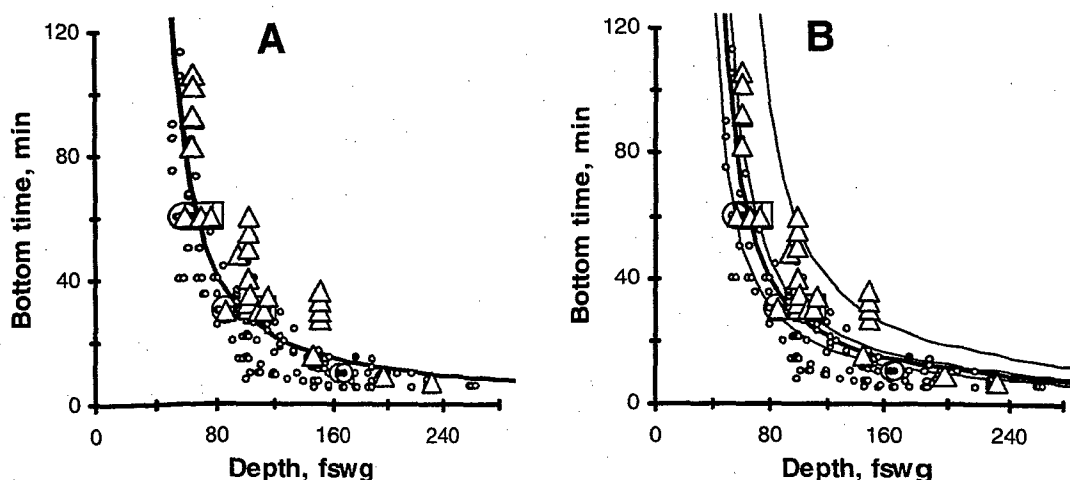


Figure 4. Dive-outcome data and probability isopleths calculated by the P-No-Stop Model. As in Figure 3, small circles = no DCS in at least one and usually several subjects, triangles = DCS cases, triangles with large circles = subjects who breathed a low FO_2 mixture, triangles with large squares = subjects who breathed a high FO_2 mixture, bull's-eye shapes = selected DCS cases from profiles that include decompression stops. A: heavy curve represents P_{DCS} of 2.0%. B: curves, from left to right: $P_{DCS} = 1, 2, 3$, and 20%.

Figures 5, 6, and 8 show correlations between predictions by the P-No-Stop Model and observations derived from subgroups of data. To produce the figures, we sorted the entire No-Stop dataset, or a subset of it, by a variable and then apportioned the person-dives into subdivisions (bins) containing approximately equal numbers of person-dives. For example, there are approximately 340 person-dives in each of the six bins in Figure 5.

In Figure 5, predicted DCS follows the observed DCS well throughout the ranges of the variables. Chi-square values for the panels are well below 11.1, the value for 95% confidence and 5 degrees of freedom: 1.1 (panel A), 2.9 (panel B), and 3.9 (panel D). For statistical analysis, it is desirable to have even distribution of incidences over the

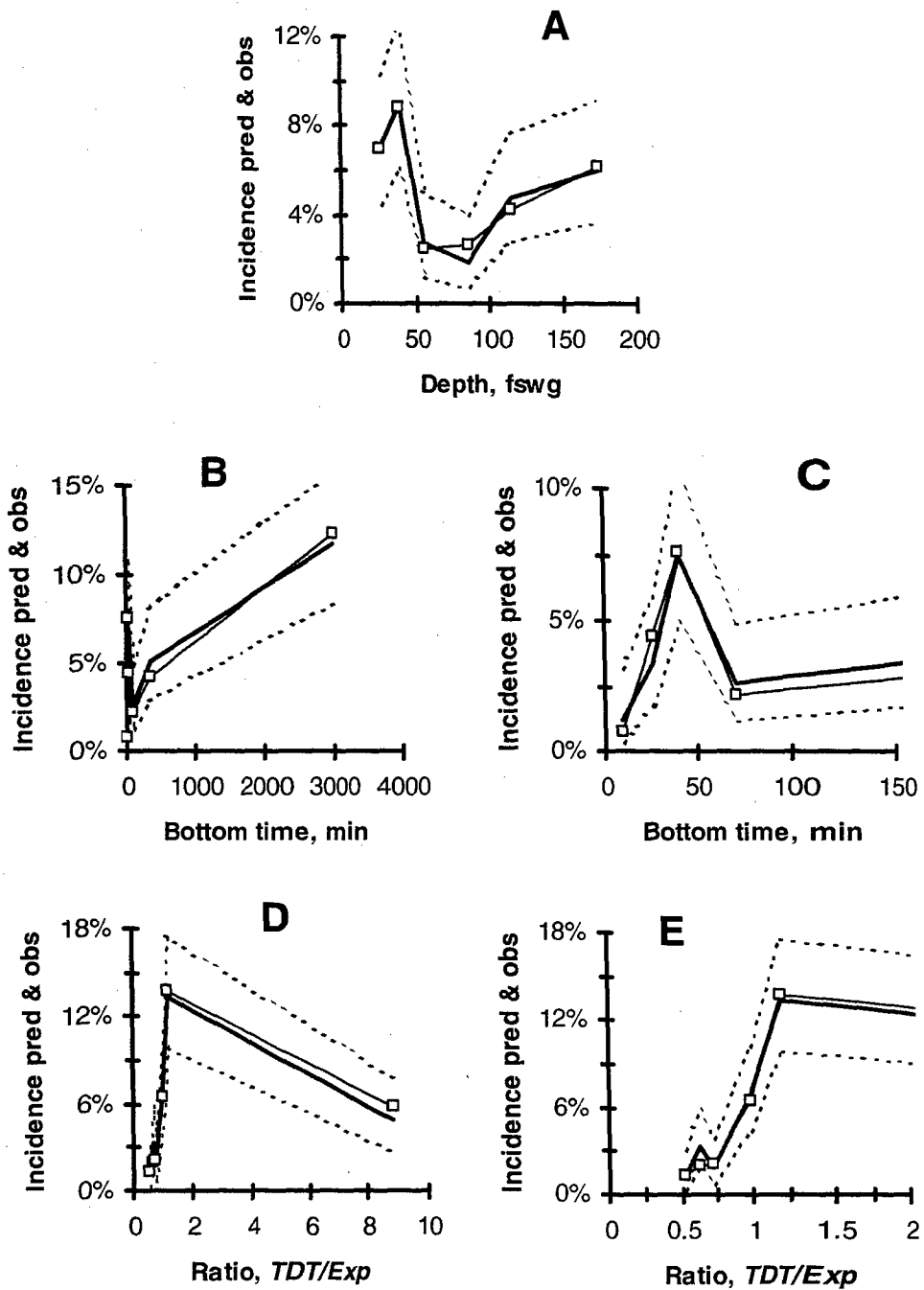


Figure 5. Incidences of DCS as functions of a variable: observed (squares and light traces) and predicted (heavy traces). Dashed traces show 95% confidence intervals of observed DCS cases. A: X-axis is the average depth in the bin. B: X-axis is the average bottom time on a scale that covers all the data. C: short bottom-time region is amplified. D: X-axis is the ratio of actual TDT to the TDT expected with an ascent of 30 fsw/min; extreme right-hand points include saturation dives, which we accepted for the calibration dataset even though they have long TDTs. E: low-ratio region is amplified.

ranges of the variables. In Figure 5A, predicted and observed DCS incidences as functions of depth fluctuate markedly on either side of the overall 5.1% incidence in the dataset. In Figure 5B, the incidences range from less than 1% to more than 12%. The bottom-time scale in Figure 5B is large enough to show a bin that contains saturation data at the right; as a consequence, the other points are squeezed against the Y-axis. In Figure 5C, the short-dive region is amplified; incidence is low for dives with short bottom times. In later sections we discuss evidence that deep no-stop dives are not as safe as this low incidence suggests.

Figures 5D and 5E shed additional light on the poor distribution of the TDT/Exp ratio in Figure 2C. Incidence is very low when the ratio is near 0.5 (for an ascent rate of 60 fsw/min) and high when the ratio is near 1.0 (for an ascent rate of 30 fswg/min). When we divide the nonsaturation person-dives according to TDT/Exp ratio, we find 1,055 dives with the ratio between 0.5 and 0.74 (average $TDT/Exp = 0.6$ with observed incidence of 2.3%) and 800 dives with the ratio between 0.75 and 1.5 (average $TDT/Exp = 1.1$ with observed incidence of 8.9%). Thus, dives with ascent rates around 30 fsw/min have incidence almost four times higher than dives with 60 fsw/min rates. To test the hypothesis that slow ascents are dangerous, we added a term containing the TDT/Exp ratio to the Equation 4 *LOGIT* function. The result indicates that a 30 fsw/min ascent rate may actually be safer than a 60 fsw/min rate, but the result is not statistically significant. We conclude that the high incidence seen near a ratio of 1.0 in Figures 5D and 5E probably results from a preponderance of aggressive dive profiles (that is, dives that are long and deep) in the 30 fsw/min group, not from ascent rate itself.

We generate Figure 6 from the No-Stop calibration data by forming bins according to estimated P_{DCS} and then plotting observed DCS for a bin against incidence predicted by the P-No-Stop Model for that bin. Solid lines and curves on the graphs are drawn by least-squares; equations for the trends and R^2 values appear in boxes. The equations refer to probability fractions rather than to percentages. The person-dives are clustered in four of the five bins with DCS incidence less than 5%, and three of the bins have observed incidence less than 2%. Observed and predicted outcomes are highly correlated. Chi-square is 2.81 for the points in Figure 6A, well below the chance value of 9.49 for 95% confidence for 4 degrees of freedom.

In the low probability range (Figure 6B), agreement is fair: for the data point with predicted incidence of 1.26%, observed incidence is 1.23%, but the other points deviate from the identity line. In other work we recommend adjusting or fine-tuning a probabilistic model when the low-incidence range appears to have a systematic bias.²⁴ The box contains the equation for the curve drawn by least squares through the data points. According to the curve and to this equation, observed incidence is 1.71% when predicted incidence is 2.0% and observed incidence is 1.0 when predicted incidence is 0.64%. The differences between predicted and observed incidences in Figure 6B appear to be systematic, so we judge that applying the fine-tuning process may be appropriate for the P-No-Stop Model. The crux of the process is to substitute the "probable incidence," defined as the average observed incidence calculated by the least-squares trend curve, for the predicted incidence.

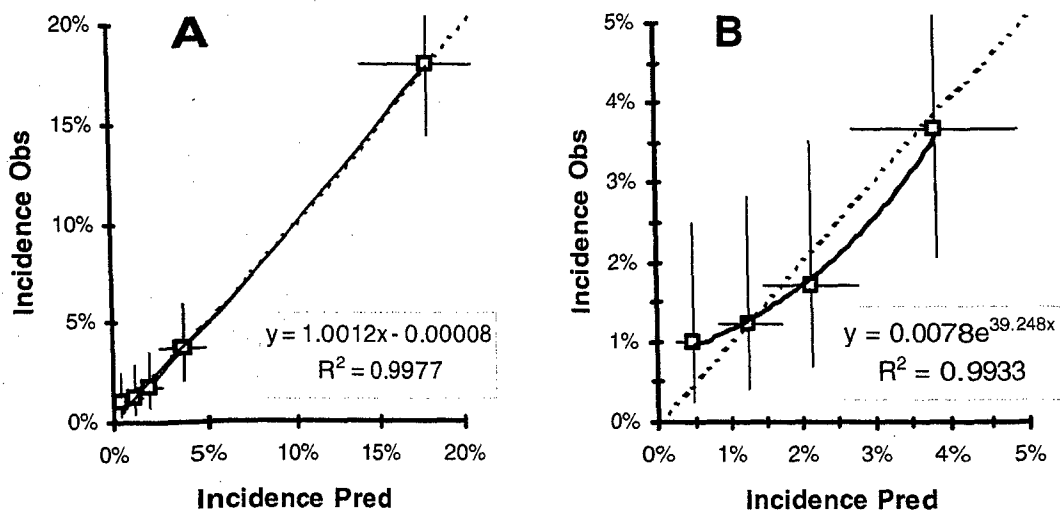


Figure 6. Observations (DCS cases/100 person-dives) vs. P-No-Stop Model predictions within approximately equal subdivisions of the calibration data. Dashed lines are identity lines. Horizontal and vertical lines show 95% confidence intervals around the predicted and observed incidences. A: all the calibration data; the solid line is the least-squares line (see the equation in the box). B: low-incidence points from Panel A; the solid curve is the least-squares curve for the 4 points (see the equation in the box).

Goodness of fit, subsaturation dives

Figure 7 shows P_{DCS} isopleths in the subsaturation range (arbitrarily defined as bottom times between 240 and 1,440 min) for the no-stop probabilistic model. Clearly the estimates are beyond the range of the data except for relatively deep subsaturation dives and for dives with high P_{DCS} . There are no dives at all in the calibration dataset for depths shallower than 20 fswg, and no DCS cases shallower than 23 fswg. Almost all the dives in the box have high estimated P_{DCS} , so P_{DCS} estimates less than 5% tend to be extrapolations from regions where the bulk of the calibration data lie.

The two dashed vertical line segments at the top of Figure 7 show 1% P_{DCS} (left) and 2% P_{DCS} (right) predicted by a model based on Equation 4 but using saturation dives only.¹⁴ The P-No-Stop Model curves for 1 and 2% P_{DCS} match up well with their counterparts from the other model.

For an example of the relation between the P_{DCS} isopleths and DCS incidences, consider the 20% P_{DCS} curve in Figure 7. The curve passes through two groups of triangles: (1) a group with bottom times of 1,440 min with depths between 26 and 38 fswg represents 8 DCS cases; there are 25 person-dives at 1,440 min, so the average incidence is 32%, and (2) a group with 720 min bottom time between 31 and 41 fswg represents 23 DCS cases; there are 118 person-dives at 720 min, so average incidence is 19.5%. Thus, the groups have appropriate incidences to be near the 20% isopleth.

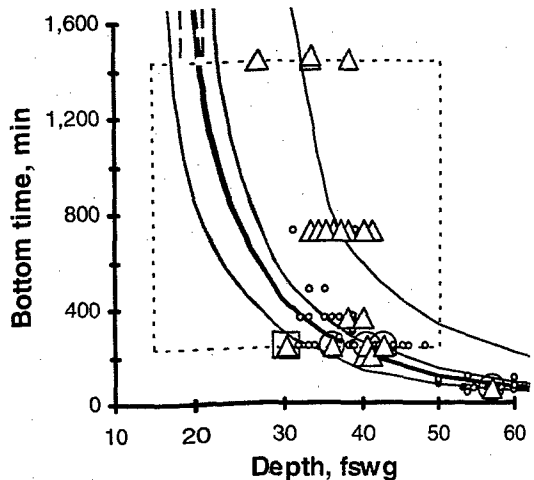


Figure 7. Probability isopleths for the P-No-Stop Model (solid curves) for shallow dives. The dashed box outlines the region of subsaturation dives. The P_{DCS} values are, from left to right, 1, 2, 3, and 20%. Symbols are as in Figure 3. Dashed vertical line segments at the top left of the graph are for 1 and 2% P_{DCS} according to a model based only on saturation dives.

three bins centered at 30, 35, and 40 fswg. The Figure 8 list of averages of depths and bottom times for the seven bins that result can be compared with Figure 7. No subsaturation dives are shallower than 30 fswg in the dataset. The Figure 8 graphs show that the No-Stop probabilistic model fits well with the limited data available: the chi-square for Figure 8A is 1.4, and 12.6 is the tabulated value for 95% confidence and 6 degrees of freedom.

DETERMINISTIC MODEL

In Figures 9, 10, and 11, the traces often lie close to each other, making it difficult to distinguish one from the others. This is an important point: the various options for no-stop dives do not differ from each other significantly, if we consider the inherent uncertainty in modeling dive-outcome data. Figure 9 shows how the models differ from each other in an important way only with deep, short dives. The top panels in Figure 9 show symbols for dive-outcome data along with our models' options for no-stop instructions. The bottom panels illustrate the relationship of our models to the current U.S. Navy no-stop instructions and the uncertainty involved in our estimates.

In Figure 9A the beaded trace for 1% P_{DCS} according to our No-Stop probabilistic model avoids all triangles and bull's-eye symbols except for a triangle inside a large square at 30 fswg. As in Figure 3, we drew the solid heavy curve for our deterministic model by

In Figure 7 only two triangles are below or to the left of the isopleth for 1% P_{DCS} . One is at an equivalent depth of 30 fswg and bottom time of 240 min, with a square around it to signify that it is one of the points for breathing gas having FO_2 above that of air [case number (1) in Table 2]. The other, at the lower-right corner of the graph, is for two DCS cases superimposed on each other at an equivalent depth of 57 fswg with bottom time of 60 min. The circle around it signifies that it is for breathing of FO_2 below that of air [cases (2) and (3) in Table 2]. Several triangles are below or to the left of the curve for 2% P_{DCS} .

To probe the fit of the P-No-Stop Model in the subsaturation range, we sort the dives in the No-Stop spreadsheet by depth after excluding dives with bottom times of 1,440 min or longer (saturation dives). From the shallow dives in the sorted set, we produce

The bins for 35 and 40 fswg contain enough person-dives that it is feasible to sort them again by bottom time to make additional bins. The Figure 8 list of averages of depths and bottom times for the seven bins that result can be compared with Figure 7. No subsaturation dives are shallower than 30 fswg in the dataset. The Figure 8 graphs show that the No-Stop probabilistic model fits well with the limited data available: the chi-square for Figure 8A is 1.4, and 12.6 is the tabulated value for 95% confidence and 6 degrees of freedom.

Depth, fswg	Bottom time, min	Observed Incidence	Predicted Incidence	Person- Dives
30.8	291	2%	1%	43
35	281	2%	2%	65
35.4	720	14%	14%	64
38.9	348	6%	5%	54
39.5	720	27%	30%	52
40.2	240	2%	3%	60
40.4	200	3%	2%	103

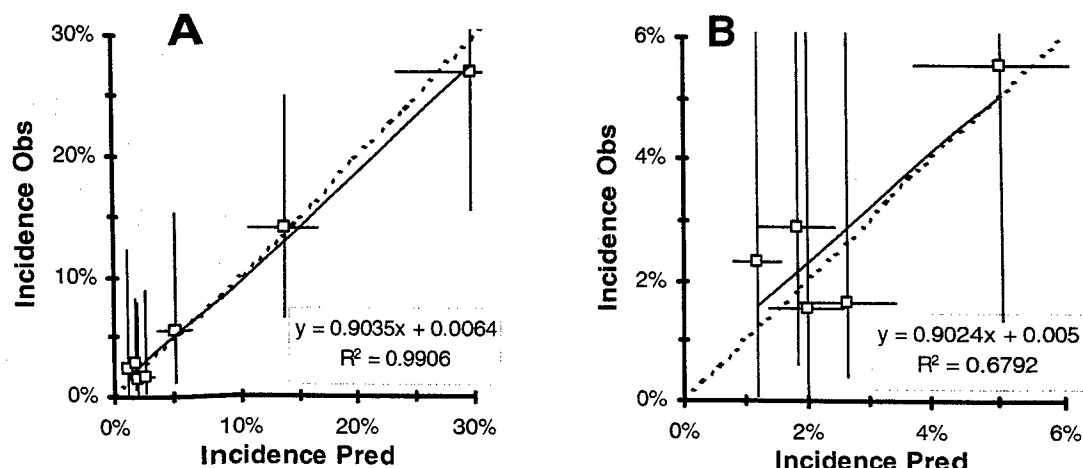


Figure 8. Subsaturation dives: incidences observed and predicted; the inset lists the divisions of the data plotted. Sloping solid lines are trend lines with accompanying equations. Horizontal and vertical lines are 95% confidence intervals around the predicted and observed DCS incidences. Dashed lines are identity lines. A: all points in the inset list. B: five lowest incidences in the inset list.

eye: it tends to superimpose on the 1% P_{DCS} trace for the P-No-Stop Model at the right of Figures 9A and 9C and also at the left of Figures 9B and 9D. In Figure 9B the middle part of the D-No-Stop Model has many circles below it, evidence that the location of the D-No-Stop curve appropriately divides DCS cases from non-DCS cases.

The important feature of Figure 9 is that the deterministic model traces deviate from the probabilistic model traces at the right of Figures 9B and 9D. In avoiding triangles and bull's-eye symbols on the right side of Figure 9B, the D-No-Stop Model allows considerably less bottom time than the No-Stop curves for 1% and 2% P_{DCS} . The DCS cases that cast doubt on the safety of the beaded P-No-Stop Model prescriptions at the right-hand side of Figure 9B are the lowest bull's-eye point (165 fswg, bottom time of 10 min, 2 DCS cases) and two triangles (198 fswg, bottom time of 9 min, 1 DCS case; and 231 fswg, bottom time of 6.8 min, 2 DCS cases).

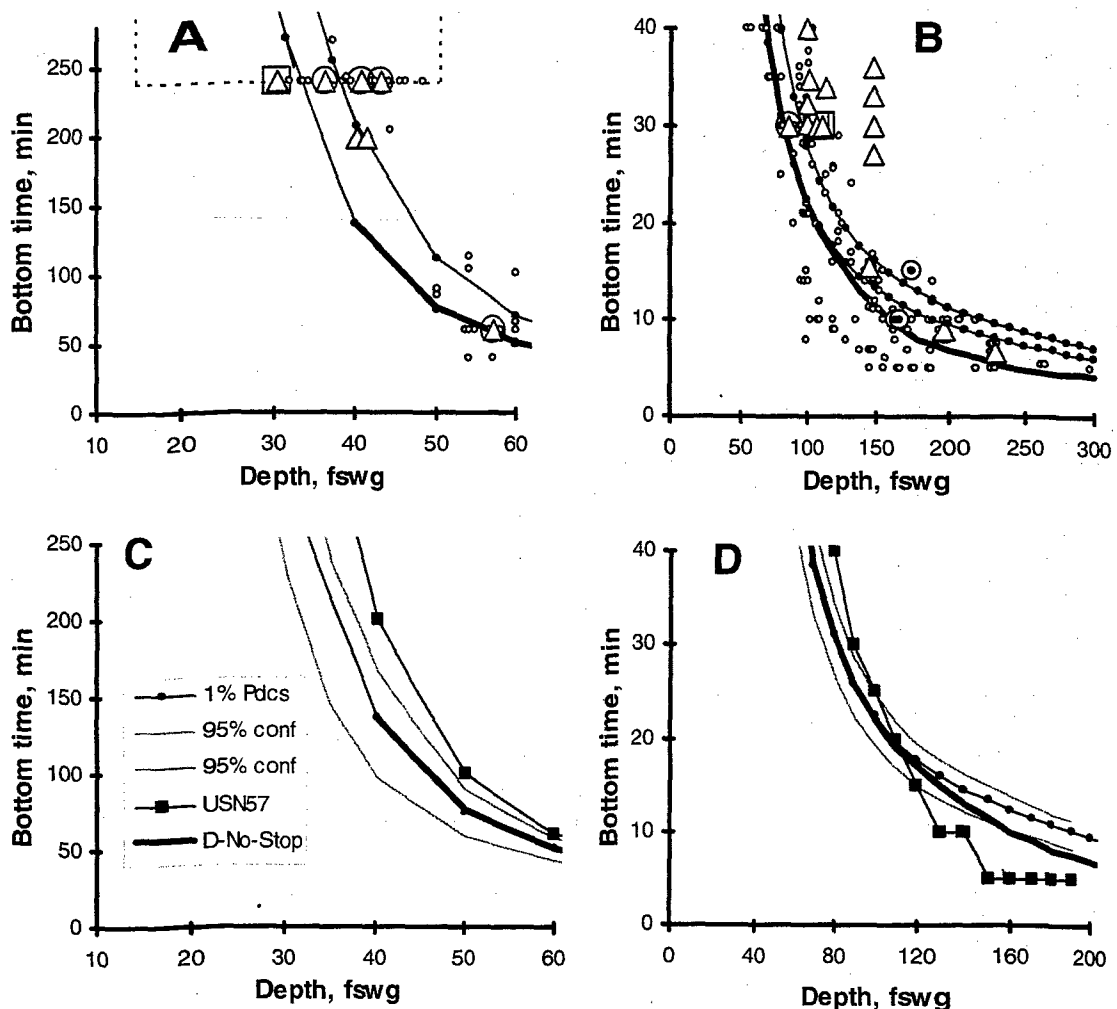


Figure 9. The deterministic D-No-Stop Model (heavy traces that go no higher than 140 min) compared with isopleths for 1 and 2% P_{DCS} (beaded traces) for the probabilistic P-No-Stop Model. Symbols are as in Figure 3. A and C: shallow dives; B and D: deep dives. A: the dashed box shows the bottom of the subsaturation range seen in Figure 7; at the lower right, the probabilistic No-Stop Model's 1% P_{DCS} curve is obscured by the D-No-Stop curve. B: for deep dives, the deterministic model deviates from two traces for the probabilistic model. C: the 95% confidence intervals (gray) around the probabilistic model's estimate of 1% P_{DCS} ; the trace with black squares is for USN57; the probabilistic model's trace for 2% P_{DCS} is omitted to reduce clutter. D: as in panel C, for deep dives.

The bottom times permitted by the P-No-Stop Model for depths between 140 and 190 fswg are as much as twice as long as those for the D-No-Stop Model. The USN57 trace, also deterministic, is close to the No-Stop 2% curve at the left of Figure 9D but falls below the 1% trace at the right.

The 1% curve for the P-No-Stop Model and the D-No-Stop Model give similar prescriptions where the probabilistic model is successful in Figure 9, at depths from 40 through about 130 fswg. However, for no-stop dives deeper than 130 fswg and 1% P_{DCS} (right side of Figures 9B and 9D), the deterministic model calls for much shorter

bottom times than the P-No-Stop Model. Our interpretation is that the probabilistic model fails for deep no-stop dives whereas the deterministic model, which avoids DCS cases, is appropriate. Furthermore, we speculate that P_{DCS} for the D-No-Stop Model may be about 1% for dives deeper than 130 fswg.

The uncertainty in our modeling is illustrated by the 95% confidence intervals in Figures 9C and 9D, which cover a span that is about the same as the difference between the different curves in Figures 9A and 9B. In Figure 9D the D-No-Stop trace just crosses the lower confidence boundary at the extreme right. However, the confidence interval boundaries do not include the USN57 trace at the right of Figure 9D.

We generated our model for standard air diving, the StandAir Model,¹³ from a large calibration dataset: 45% of the dives were no-stop dives, essentially those in the calibration dataset for our present models, and 55% were dives with decompression stops. Figure 10 compares traces in Figure 9 with traces for the StandAir Model and for a deterministic model known as the VVal-18 Algorithm,^{25,26} which gives TDTs for dives having decompression stops similar to those for our StandAir Model.

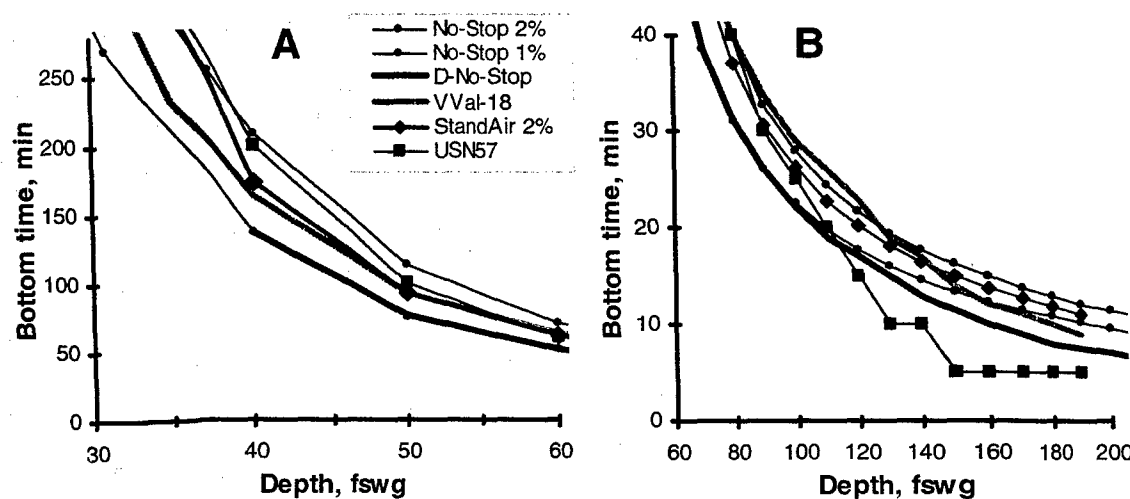


Figure 10. Traces for the StandAir Model and the VVal-18 Algorithm added to those seen in Figure 9. A: shallow dives; deeper than 40 fswg, the probabilistic P-No-Stop Model's 1% P_{DCS} curve is partly obscured by the D-No-Stop curve. B: deep dives.

- In Figure 10A the 2% P_{DCS} trace for the StandAir Model and the VVal-18 trace lie between the 1% P_{DCS} trace (hidden at the right by the D-No-Stop trace) and 2% P_{DCS} traces for the P-No-Stop Model (beaded) and StandAir Model (diamond symbols).
- At the left of Figure 10B, the gray trace for the VVal-18 Algorithm corresponds to about 2% P_{DCS} , according to the P-No-Stop Model, and the StandAir Model falls to the left of the P-No-Stop Model for 1% P_{DCS} . At the right of Figure 10 B, the VVal-18 trace is slightly below the probabilistic traces, and the trace for the USN57 instructions is far below all the other traces.

- The most important aspect of Figure 10B is at the right-hand side: the 2% trace for the StandAir probabilistic model falls between the two beaded traces for our No-Stop probabilistic model and well above the trace for our D-No-Stop Model.

DISCUSSION

NO-STOP LIMITS OF OTHER NAVIES

Table 4 lists current no-stop instructions for operational tables used by navies of Great Britain,¹⁰ Canada,¹¹ France,¹² and the United States.¹ The USN57 tends to allow longer bottom times than the other navies' tables, which tend to be similar to each other. Information from our two models appears at the right of Table 4.

TABLE 4. NO-STOP TIME LIMITS (MIN) ADOPTED BY SEVERAL NAVIES AND OUR NO-STOP MODELS

Depth fsw	Depth msw	Britain	Canada	France	USN57	No-Stop 1% Pdcs	No-Stop 2% Pdcs	D-No- Stop
10	3	U	U	U	U	U	U	--
15	--	U	U	U	U	U	U	--
20	6	U	U	U	U	855	1,733	--
25	--	U	--	U	595	462	694	450
30	9	U	300	360	405	294	429	300
35	--	--	--	270	310	198	293	200
40	12	120	150	165	200	137	208	137
50	15	75	75	80	100	75	112	76
60	18	55	50	50	60	51	70	51
70	21	35	35	35	50	38	51	38.5
80	24	28	25	25	40	31	40	31
90	27	22	20	20	30	26	33	26
100	30	18	15	15	25	22	28	22
110	33	15	12	12	20	20	24	19
120	36	12	10	10	15	18	22	17
130	39	8	8	8	10	16	19	15
140	42	7	7	7	10	15	18	13
150	45	6	6	6	5	13	16	11.5
160	48	0	6	5	5	12	15	10
170	51	0	5	5	5	12	14	9
180	54	0	5	0	5	11	13	8
190	57	0	5	0	5	10	12	7.5

U = unlimited time at depth is allowed
-- = no entry

Using the format introduced in previous figures (shallow no-stop dives in left-hand panels and deep no-stop dives in right-hand panels), Figure 11 compares the information in Table 4. In Figure 11A, the USN57 trace is a little below the 2% P_{DCS} curve for the P-No-Stop Model. Except for USN57, the navy traces tend to be a little above or on the 1% P_{DCS} trace; apparently, the no-stop prescriptions of the British, Canadian, and French navies reflect risks near 1% for depths shallower than 100 fswg.

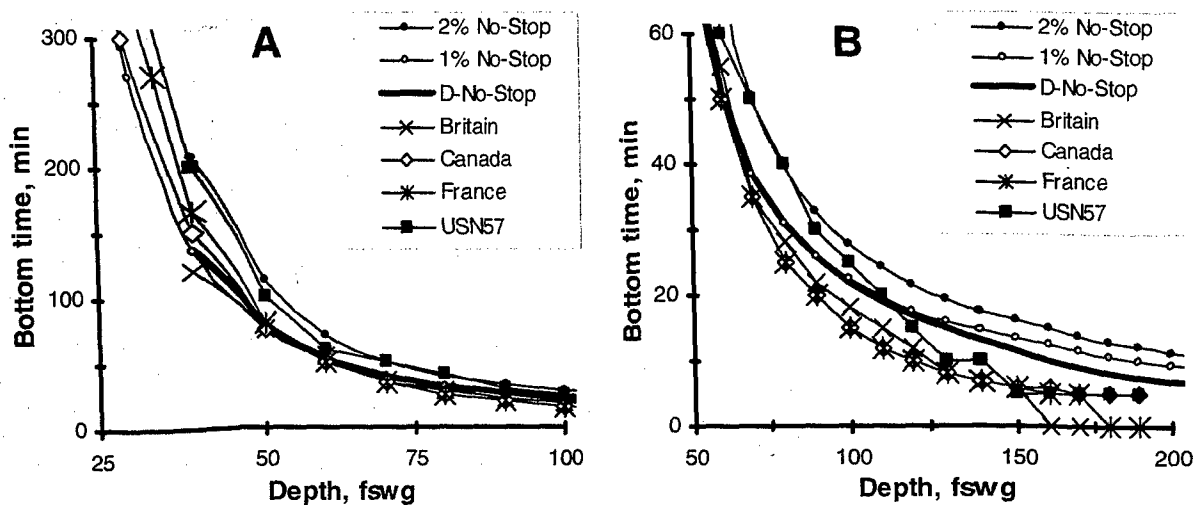


Figure 11. No-stop times for various navies plus our deterministic D-No-Stop Model (heavy trace) and isopleths for our No-Stop probabilistic model (beaded curves for 2% P_{DCS} (upper) and 1% P_{DCS} (lower)). In both panels, USN57 is the trace with black squares. A: shallow dives. B: deep dives.

For deep dives, the differences between our P-No-Stop Model and the navy instructions in Figure 11B are large; all the navy traces mandate much shorter bottom times than do the beaded traces for our probabilistic model. The D-No-Stop trace is between the traces for the other navies and the traces for the probabilistic model. For example, Table 4 and the right side of Figure 11B show that the allowed bottom times for no-stop dives to 190 fswg are 10 and 12 min for the probabilistic P-No-Stop Model, 7.5 min for the D-No-Stop Model, and 5 min for USN57 and Canada; dives to 190 fswg are not allowed by British and French navies.

Figure 12 shows that estimates of P_{DCS} calculated with our P-No-Stop Model tend to be 1.5% to 2% for the USN57 schedule for depths shallower than 100 fswg. The uncertainty of the USN57 estimates is illustrated by the two varying dashed traces for upper and lower 95% confidence intervals. Another aspect of uncertainty involves the two dashed horizontal traces: the least-squares trend curve in Figure 6 shows that when P_{DCS} is 1%, average observed incidence or "probable incidence" is 0.64%, and when P_{DCS} is 2%, probable incidence is 1.71%. Thus, the probable incidence associated with the upper horizontal line in Figure 12 is 1.71%, and the probable incidence for the lower horizontal trace is 0.64%.

In Figure 12 the other navies tend to have P_{DCS} around 1%, or less than 2% for depths shallower than 100 fswg, and confidence intervals around their traces (not shown) are

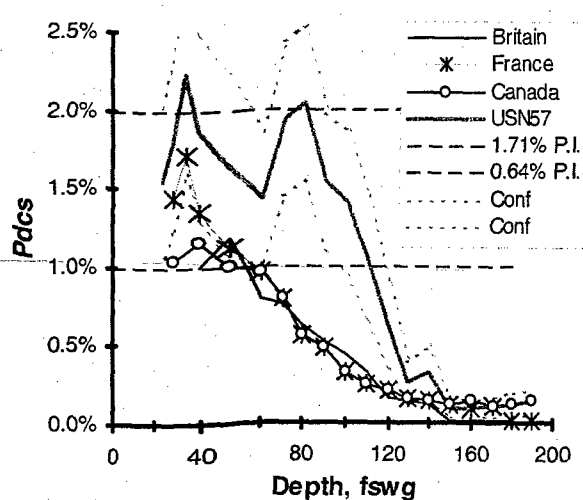


Figure 12. P_{DCS} estimates for no-stop times, calculated by our No-Stop probabilistic model. Irregular dashed traces show the 95% confidence intervals for USN57. The dashed horizontal line segments show "probable incidences," which are less than the P_{DCS} for the same location.

similar to the intervals for the USN57 Model. If the P-No-Stop Model is faulty for deep dives, its estimates of P_{DCS} for the right side of Figure 12B are incorrect.

PITFALLS IN PROBABILISTIC MODELING

Figures 9B, 9D, 10B, and 11B illustrate a discrepancy between deterministic and probabilistic models: the bottom times prescribed for deep, no-stop dives by the deterministic D-No-Stop Model and the operational navies are considerably shorter than the bottom times prescribed by the probabilistic P-No-Stop and StandAir models. Our interpretation is that the probabilistic models are at fault. We recognize three general pitfalls in probabilistic modeling.

Inappropriate equations

The first pitfall is that the equation used to fit the data may introduce bias. The simple analogy here is that it is undesirable to fit a least-squares straight line to points that appear as a curve on a graph, and any applications of the parameter values derived from such a fit are misleading. The inappropriate equation prevents the model from providing a good fit to the data points in certain regions.

Our use of Equation 4 presumes that the combination of two compartments, one of them weighted, acceptably represents a continuum of many critical compartments having varying halftimes. However, the halftimes of 21.5 and 420 min found by the statistical process can be expected to provide questionable results for deep dives; for such dives, bottom times are comparatively short, so the model should probably include a compartment with halftime shorter than 21 min. When we generated a three-exponential model with two of the exponential terms weighted, one of the halftimes was 11 min. We also tested models with a third exponential term having halftimes fixed at 6, 3, or 1 min. However, for all these, the LL was not better than that for Equation 4, and the prescriptions for deep, short dives were not significantly better than those of the P-No-Stop Model. Apparently the lack of deep, short dives in the dataset is more troublesome than is the lack of a compartment with a short halftime.

Out-of-bounds data

A second pitfall in probabilistic modeling concerns the quality of the calibration data. The practical value of the model is compromised if the data are not representative of the intended use of the model. Our calibration dataset provides an unavoidable example of this defect. The P-No-Stop Model is intended for use with dives having the current U.S. Navy ascent rate of 30 fsw/min, but about half the calibration dives have an ascent rate of 60 fsw/min; these 60 fswg/min dives are "out-of-bounds" data. If rapid ascents are more hazardous than slow ascents, the resulting bias is on the side of safety. Some of the saturation dives have ascent rates slower than 30 fsw/min, but this slow rate may not be troublesome if the DCS bubbles that occur after saturation dives are only in compartments with very slow halftimes.

Including data beyond the range of the desired outcome invites error: the out-of-bounds data may distort the fit in the desired region. In this report our region of interest includes no-stop dives ranging from the few minutes of bottom time that are appropriate for a 190-fswg, no-stop dive to the days-long bottom times for saturation dives. Such a wide region of interest has merit for deriving prescriptions for subsaturation dives, where data are scarce, because the subsaturation region is interpolated between standard air dives and saturation dives.

In another study we tested our contention that the calibration data used to produce a model should be limited to the types of dives with which the model is to be used.²⁷ We produced a model that included both saturation and nonsaturation dives with, in both cases, decompression stops. For prescriptions of TDTs, this combination model was clearly inferior to an alternative model based on a dataset that excluded saturation dives.

This report allows a second test of our contention that out-of-bounds data can bias a model. Figure 10 shows curves for 1% and 2% P_{DCS} for no-stop dives according to our previous StandAir Model,¹³ which was generated from a database that contained approximately equal numbers of no-stop dives and dives with decompression stops. Thus, so far as no-stop dives are concerned, the StandAir Model contains out-of-bounds dives having decompression stops. However, the StandAir Model prescribes essentially the same no-stop depths and bottom times for 2% P_{DCS} as our P-No-Stop Model prescribes. This agreement between models indicates that including the out-of-bounds dives that have decompression stops does not unduly bias the no-stop predictions of the StandAir Model. The agreement between the two models is not as good for P_{DCS} of 1% as it is for P_{DCS} of 2%.

Balance

The third pitfall concerns the balance of the calibration data. The poor balance of the available data is illustrated in Figures 2 and 5. In Figure 2A, person-dives are scarce, and DCS incidence is low for deep dives. Figure 5A, with bins containing approximately equal numbers of person-dives, gives another perspective: the incidence of DCS is low

for dives around 50 to 100 fswg. The poor distribution of bottom times is manifested in Figures 2B, 5B, and 5C. Figure 2B shows that the numbers of person-dives (main figure) and incidence (inset) differ widely between bins; Figure 5B has a peak of DCS incidence for saturation dives; and Figure 5C has another peak around 40 min and very low incidence below 30 min. Figure 2C shows that ascent rate, characterized by the TDT/Exp ratio, is very unevenly distributed, especially with respect to DCS incidence (inset of Figure 2C and Figures 5D and 6E), but ascent rate does not directly affect the P-No-Stop Model because Equation 4 does not include ascent rate or TDT as a variable. Although thousands of dives are recorded in the U.S. Navy Decompression Database,^{4,5} our models are weakened by lack of data in particular depth/bottom-time regions such as saturation dives (only 246 dives with 22 DCS cases, none at depths shallower than 23 fswg), subsaturation dives (no dives at all between 720 and 1,400 min bottom times), and deep dives.

Data determine the outcome of the statistical process, of course, and depth/bottom-time regions that include many data points have more impact on the model's parameters, and therefore on the model's prescriptions, than do regions that include few points. It follows that the probabilistic fitting of poorly balanced data may give faulty estimates in some regions of interest. In regions where data are scarce, the model's output is biased by regions that contain more data. If no data are in a region, the model's output for that region is interpolated or extrapolated from regions where dive outcome information is plentiful. Outer ranges of a variable — such as the shallowest and deepest dives, dives with the shortest or longest bottom times, and dives with the lowest or highest P_{DCS} — are especially vulnerable to suboptimal fitting equations and poorly balanced data. Accordingly, our results show that the P_{DCS} estimates given by our P-No-Stop Model are questionable for the deepest dives.

A partial remedy for lack of data is to seek guidance from outside sources. One type of outside source is the operational navy tables discussed under the heading **NO-STOP LIMITS OF OTHER NAVIES**; the navies prescribe shorter bottom times for deep dives than our probabilistic model prescribes. A second outside source of information is our use of selected individual dives with decompression stops (bull's-eyes in the figures) with our deterministic models to attempt a partial compensation for the paucity of DCS cases in deep no-stop dives.

TABLES OF DCS PROBABILITY

In Tables 5 through 8 our recommendations appear in heavy boxes. Information outside the heavy boxes allows comparisons between models. The recommendations are essentially arbitrary and based on presently available data; future developments may modify or reverse them.

- We recommend prescriptions and P_{DCS} estimates given by the P-No-Stop Model for subsaturation dives and for standard dives shallower than 140 fswg.

- For no-stop dives deeper than 130 fswg, we recommend the prescriptions of the D-No-Stop Model — which, we speculate, represents P_{DCS} near 1%. We judge that our probabilistic model does not give acceptable prescriptions and appropriate P_{DCS} estimates deeper than 130 fswg.

Standard air no-stop dives: Table 5

The upper heavy box in Table 5 lists no-stop bottom times for P_{DCS} of 1%, 2%, and 3% with an ascent rate of 30 fswg/min, according to our P-No-Stop Model. The 2% P_{DCS} no-stop times in Table 5 are longer than the USN57 no-stop bottom-time limits in force in the year 2004 for all depths except 35 fswg. The USN57 bottom times are in the range of 1% and 2% P_{DCS} , according to the P-No-Stop Model, except for dives to 110 fswg and deeper, where the USN57 times are shorter than those given for 1% P_{DCS} in the table.

TABLE 5. NO-STOP TIME LIMITS (MIN): THE U.S. NAVY DIVING TABLE (USN57), THE P-NO-STOP MODEL, AND THE D-NO-STOP MODEL

Heavy boxes indicate our recommended bottom times.
Light solid boxes = bottom times less than those for USN57.
Light print = questionable values.

Depth, fswg	<u>USN57</u>	<----- Bottom times, min ----->			D-No-Stop	<i>P_{DCS}</i> for D-No-Stop	(7)
		(1) 1%	(2) 2%	(3) 3%			
25	595	462	694	889	450	1.0%	
30	405	294	429	527	300	1.0%	
35	310	198	293	358	200	1.0%	
40	200	137	208	257	137	1.0%	
50	100	75	112	141	76	1.0%	
60	60	51	70	86	51	1.0%	
70	50	38	51	60	38.5	1.0%	
80	40	31	40	46	31	1.0%	
90	30	26	33	37	26	1.0%	
100	25	22	28	32	22	0.9%	
110	20	20	24	27	19	0.9%	
120	15	18	22	24	17	0.9%	
130	10	16	19	22	15	0.8%	
140	10	15	18	20	13	---	
150	5	13	16	18	11.5	---	
160	5	12	15	16	10	---	
170	5	12	14	15	9	---	
180	5	11	13	14	8	---	
190	5	10	12	13	7.5	---	

For dives deeper than 130 fswg, we believe our No-Stop probabilistic model is too liberal; the bottom times in the heavy box in Table 5, column 6, are from the D-No-Stop Model. Even these are as much as two and a half times longer than times for USN57. The largest difference is at 150 fswg, where the time is 11.5 min instead of the 5 min of USN57. We recommend caution in lengthening no-stop bottom times for deep dives, because such dives, at least in animal studies, have been associated with DCS signs and symptoms that are more serious than those occurring in shallower dives.²⁸⁻³⁰ However, when we scrutinize information about individual DCS cases in the No-Stop spreadsheet, we cannot confirm a trend for deep cases to be more serious than shallow cases.

If we read horizontally along bottom-time entries for dives deeper than 130 fswg in columns 3 to 5 of Table 5, we see that one to three minutes of change in bottom time causes a 1% change in P_{DCS} . Therefore, if the entries in column 6 represent 1% P_{DCS} , entries for dives deeper than 140 fswg in column 4 may correspond to P_{DCS} as high as 5%.

Standard air dives over a range of risk: Table 6

Table 6, which is similar to a Table 1 published in the description of the NMRI '93 probabilistic model,¹⁵ shows how bottom times increase as P_{DCS} increases. Two columns near the center of Table 6 show that the P-No-Stop Model's bottom times for 2.3% P_{DCS} are longer than NMRI '93's for the same P_{DCS} , more than 50% longer for shallow dives. At the bottom of Table 6, the second set of entries for depths from 140 through 190 fswg show the bottom times obtained from the D-No-Stop model.

Differences between the basic properties of the NMRI '93 Model and our probabilistic model are revealed by dose-response curves. In Figure 13, traces for our P-No-Stop Model have sharper elbows than traces for the NMRI '93 Model, so that the curves for the two models tend to cross each other. The horizontal line segments in each panel show the 2.3% level of risk deemed acceptable by developers of the NMRI '93 Model. The horizontal line segment in the 40 fswg panel shows that the P-No-Stop Model allows a considerably longer bottom time than the NMRI '93 Model allows for the same P_{DCS} , and the vertical line segment shows that NMRI '93 requires a bottom time equivalent to only about 1% risk, according to the P-No-Stop Model. The crossovers in the other panels cause the NMRI '93 Model to call for shorter bottom times than the P-No-Stop Model at low P_{DCS} , but for longer bottom times at high P_{DCS} .

Except at 40 fswg, the traces for the two models tend to be close to each other when P_{DCS} is 2 to 4% in Figure 13. The vertical line in the 180-fswg panel is for 8 min, the time our D-No-Stop Model prescribes for 180 fswg. The NMRI '93 Model curve meets the heavy vertical line at about 2% P_{DCS} , but the P-No-Stop Model meets the vertical line at a very low P_{DCS} . If the D-No-Stop Model's vertical line segment is the correct bottom time for 1% P_{DCS} at 180 fswg, the NMRI '93 Model overestimates the risk and our P-No-Stop Model underestimates it.

TABLE 6. BOTTOM TIMES (MIN) ACCORDING TO THE P-NO-STOP MODEL FOR VARIOUS DCS PROBABILITIES

Boldface columns show current U.S. Navy no-stop limits (left) and the recommendations of the NMRI '93 model (middle).

Light print = questionable values.

For depths from 140 through 190 fswg, we recommend the D-No-Stop Model bottom times listed in the heavy box at the bottom of the table.

<i>P_{DCS}</i> →	USN57	1.0%	2.0%	2.1%	2.2%	2.3%	NMRI '93 2.3%	2.4%	2.5%	3.0%	4.0%	5.0%	6.0%
Depth													
20	—	858	1,735	1,893	2,097	2,390	513	**	**	**	**	**	**
25	595	462	694	714	734	754	338	774	793	889	1083	1294	1550
30	405	294	429	440	451	461	245	471	481	527	608	680	747
35	310	197	293	300	308	315	185	321	328	358	409	453	491
40	200	137	208	214	219	224	144	229	234	257	294	325	352
45	—	99	151	155	159	163	114	167	171	188	218	242	262
50	100	75	112	116	119	122	93	125	127	141	164	183	200
55	—	61	87	89	92	94	77	96	98	108	125	141	154
60	60	51	70	72	74	75	64	77	78	86	99	110	120
70	50	38	51	52	53	54	48	55	56	60	67	74	80
80	40	31	40	41	41	42	38	42	43	46	51	55	59
90	30	26	33	33	34	34	32	35	35	37	41	44	47
100	25	22	28	28	29	29	27	30	30	32	34	37	39
110	20	20	24	25	25	25	24	26	26	27	30	32	33
120	15	18	22	22	22	22	21	23	23	24	26	28	29
130	10	16	19	20	20	20	18	20	21	22	23	25	26
140	10	15	18	18	18	18	16	18	19	20	21	22	23
150	5	13	16	16	17	17	16	17	17	18	19	20	21
160	5	12	15	15	15	15	14	16	16	16	18	19	19
170	5	12	14	14	14	14	13	14	15	15	16	17	18
180	5	11	13	13	13	13	12	13	14	14	15	16	17
190	5	10	12	12	12	13	11	13	13	13	14	15	16
140	10	13	--	--	--	--	16	--	--	--	--	--	--
150	5	11.5	--	--	--	--	16	--	--	--	--	--	--
160	5	10	--	--	--	--	14	--	--	--	--	--	--
170	5	9	--	--	--	--	13	--	--	--	--	--	--
180		8	--	--	--	--	12	--	--	--	--	--	--
190	5	7.5	--	--	--	--	11	--	--	--	--	--	--

** = more than 2,880 min

-- = no entry

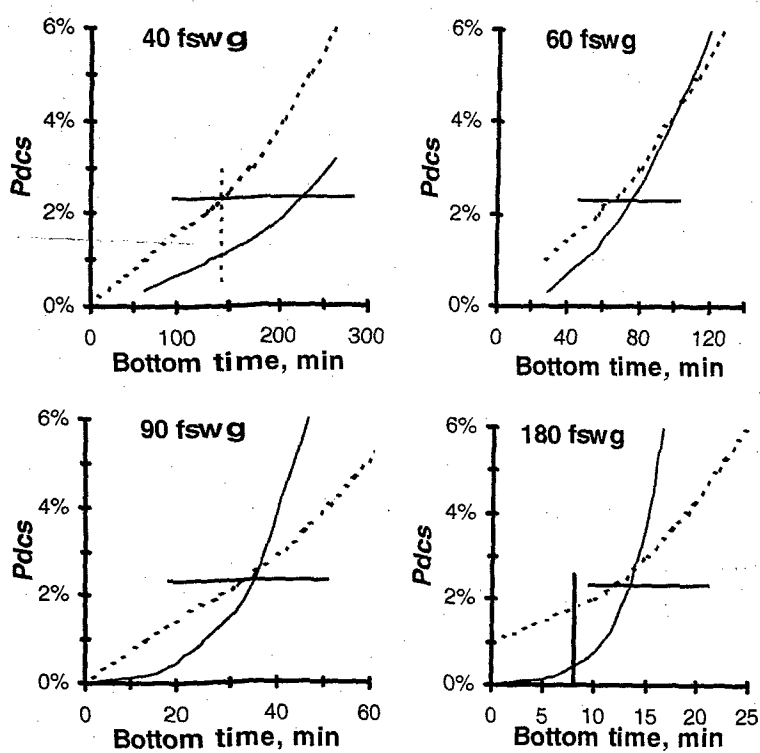


Figure 13. Dose-response curves for the P-No-Stop Model (solid curves) and the NMRI '93 Model (dashed curves) for four depths. Horizontal line segments show the no-stop times for NMRI '93. The vertical dashed line segment in the 40-fswg panel compares the two models at the same bottom time. The vertical line segment in the 180-fswg panel shows the D-No-Stop Model's bottom time.

Table 8 lists bottom times less than 2 days given by the P-No-Stop Model for subsaturation and shallow dives between 18 and 60 fswg for various *P*_{dcs} values. For example, the 2% *P*_{dcs} column shows that a bottom time of 1,735 min (29 hr) at 20 fswg and a bottom time of 694 min (11.6 hr) at 25 fswg have the same risk of DCS. The USN57 column allows 405 min (less than 7 hr) at 30 fswg, a bottom time that gives a little less than 2% *P*_{dcs}. The 1% column shows that a diver can remain at 35 fswg for 197 min (3.3 hr), and the 5% column shows that a diver can remain at 35 fswg for 453 min (7.6 hr). At 35 fswg, *P*_{dcs} is greater than 30% for a diver who makes a no-stop ascent after 1,440 min (24 hr).

Subsaturation dives: Tables 7 and 8

Table 7 lists bottom times for subsaturation dives calculated by the P-No-Stop model for 1 and 2% *P*_{dcs}. Practical experience indicates that the USN57 table is reliable in the subsaturation region.³¹ For 2% *P*_{dcs}, the P-No-Stop Model's bottom times are 17% longer than those of USN57 at 25 fswg, 5% longer at 30 fswg, and 6% shorter at 35 fswg. The upper and lower 95% confidence intervals in columns 4, 5, 7, and 8 give an idea of the uncertainty involved in the bottom times: the confidence intervals extend over 100 minutes on either side of the prescribed times at the top of the table; for 40 fswg at the bottom of the table, confidence intervals extend about a half hour from either side of the prescribed times.

TABLE 7. BOTTOM TIMES (MIN) FOR SUBSATURATION NO-STOP DIVES

Light print = interpolations between standard air dives and saturation dives due to lack of data.

Entries in light boxes = bottom times less than those for USN57.

(1)	(2)	(3)	(4)	(5)	(6)	(7)	(8)
Depth, fswg	USN57	No-Stop Model, 1% Pdcs	Low C.I.	High C.I.	No-Stop Model, 2% Pdcs	Low C.I.	High C.I.
23		572	433	693	897	715	1,083
24		512	391	616	783	630	928
25	595	462	353	552	694	566	811
26		419	322	499	622	508	722
27		381	292	452	562	462	648
28		348	266	411	511	422	587
29		319	244	377	468	387	535
30	405	294	222	347	429	357	490
31		270	205	320	396	329	451
32		249	188	297	366	304	416
33		230	172	275	339	282	386
34		213	159	255	315	260	359
35	310	197	145	238	293	242	334
40	200	137	98	168	208	167	241

CONCLUSIONS

1. Our No-Stop probabilistic model, based on all the no-stop data, gives acceptable *Pdcs* estimates for no-stop dives shallower than 130 fswg, but not for no-stop dives deeper than 130 fswg.
2. For deep no-stop air dives, our D-No-Stop model, fashioned to avoid observed cases of DCS, gives acceptable bottom times: *Pdcs* is indeterminate, but we judge it to be about 1%.
3. The P-No-Stop Model seems to give acceptable bottom-time limits for subsaturation dives, although the model results are interpolations between standard air dives and saturation dives in much of this region.
4. Our evidence that the P-No-Stop Model underestimates risk of DCS in deep dives shows that a probabilistic model that serves well for much of the depth/bottom-time region of the dataset can give faulty results in a certain region, even when such a model is based on a relatively homogeneous dataset containing only no-stop dives.

TABLE 8. SUBSATURATION DIVES AND SHALLOW DIVES: ESTIMATES OF BOTTOM-TIME LIMITS (MIN) FROM THE P-NO-STOP MODEL

+++ = bottom times of 48 hr or more

Entries in light boxes = bottom times less than those for USN57

Light print = interpolations between standard air dives and saturation dives.

Depth fswq	<u>USN57</u>	Bottom times, min							
		1%	2%	3%	5%	10%	20%	30%	50%
18		1,293	+++	+++	+++	+++	+++	+++	+++
19		1,026	+++	+++	+++	+++	+++	+++	+++
20		858	1,735	+++	+++	+++	+++	+++	+++
21		737	1,288	2,556	+++	+++	+++	+++	+++
22		646	1,053	1,561	+++	+++	+++	+++	+++
23		572	897	1,227	2,798	+++	+++	+++	+++
24		512	783	1,028	1,644	+++	+++	+++	+++
25	595	462	694	889	1,294	+++	+++	+++	+++
26		419	622	784	1,088	2,577	+++	+++	+++
27		381	562	701	945	1,664	+++	+++	+++
28		348	511	633	836	1,334	+++	+++	+++
29		319	468	576	750	1,134	+++	+++	+++
30	405	294	429	527	680	993	1,799	+++	+++
31		270	396	484	621	886	1,435	+++	+++
32		249	366	447	570	800	1,221	1,888	+++
33		230	339	414	526	729	1,072	1,499	+++
34		213	315	385	487	669	958	1,275	+++
35	310	197	293	358	453	617	868	1,120	2,135
36		183	273	334	422	572	794	1,004	1,642
37		170	255	312	394	533	731	911	1,386
38		158	238	292	369	497	677	834	1,214
39		147	222	274	346	466	629	769	1,087
40	200	137	208	257	325	437	588	714	987
41		127	195	241	306	411	550	665	905
42		119	183	226	288	387	517	622	836
43		112	171	213	271	365	487	584	777
44		105	161	200	256	345	459	549	725
45		99	151	188	242	326	434	518	680
46		93	142	178	228	309	411	490	639
47		88	134	167	216	293	390	464	603
48		83	126	158	204	278	370	440	570
49		79	119	149	193	264	352	418	540
50	100	75	112	141	183	251	334	398	512
51		72	106	133	173	238	318	379	487
52		69	101	126	164	227	303	361	464
53		66	96	120	156	215	289	344	442
54		63	91	114	148	205	276	329	422
55		61	87	108	141	195	264	314	403
56		58	83	103	134	186	252	300	385
57		56	80	98	127	177	241	287	369
58		54	76	94	121	169	230	275	353
59		53	73	89	115	161	220	263	339
60	60	51	70	86	110	154	211	252	325

PAGE INTENTIONALLY LEFT BLANK

REFERENCES

1. Commander, Naval Sea Systems Command, *U.S. Navy Diving Manual, Revision 4*, Publication SS521-AG-PRO-010 (Arlington, VA: Naval Sea Systems Command, 1999).
2. P. K. Weathersby, L. D. Homer, and E. T. Flynn, "On the Likelihood of Decompression Sickness," *J Appl Physiol*, Vol. 57 (1984), pp. 815–824.
3. E. C. Parker, S. S. Survanshi, P. B. Massell, and P. K. Weathersby, "Probabilistic Models of the Role of Oxygen in Human Decompression Sickness," *J Appl Physiol*, Vol. 84 (March 1998), pp. 1096–1102.
4. D. J. Temple, R. Ball, P. K. Weathersby, E. C. Parker, and S. S. Survanshi, *The Dive Profiles and Manifestations of Decompression Sickness Cases after Air and Nitrogen-Oxygen Dives*, NMRC Technical Report 99-02, Naval Medical Research Center, May 1999.
5. P. K. Weathersby, S. S. Survanshi, R. Y. Nishi, and E. D. Thalmann, *Statistically Based Decompression Tables VII: Selection and Treatment of Primary Air and N₂O₂ Data*, Joint Technical Report, NSMRL #1182 and NMRI 92-85, Naval Medical Research Institute, Sept 1992.
6. D. R. Leitch and E. E. P. Barnard, "Observations on No-Stop and Repetitive Air and Oxynitrogen Diving," *Undersea Biomed Res*, Vol. 9 (June 1982), pp. 113–129.
7. J. A. Hawkins, C. W. Shilling, and R. A. Hansen, "A Suggested Change in Calculating Decompression Tables for Diving," *US Navy Med Bull*, Vol. 33 (1935), pp. 327–338.
8. O. E. Van der Aue, R. J. Kellar, E. S. Brinton, G. Barron, H. D. Gilliam, and R. J. Jones, *Calculation and Testing of Decompression Tables for Air Dives Employing the Procedure of Surface Decompression and the Use of Oxygen*, NEDU Report No. 1, Navy Experimental Diving Unit, 1951.
9. G. Albano, "Experimental Research on the Decompression of Man: I. Critical Safety Values of the Pressure Gradient during a Direct Ascent to the Surface without Stops," *Med dello Sport*, Vol. 1 (1961), pp. 259–275.
10. *U.K. Military Diving Manual, Volume II, Change I, Book of Reference 2806* (Fareham, Hants, U.K: Commander in Chief, Fleet, 2001).
11. G. R. Lauckner and R. Y. Nishi, *Canadian Forces Air Decompression Tables*, Report No. 85-R-03 (Downsview, Ont., Canada: Defence and Civil Institute for Environmental Medicine, 1985).

12. J. L. Méliet, *Les Tables de Plongée à l'Air de la Marine National: Historique, Étude Statistique, Propositions d'Amélioration*, Procès-verbal No. 03/90 (Toulon Naval, France: Commission d'Études Pratiques d'Intervention Sous la Mer, 1990).
13. H. D. Van Liew and E. T. Flynn, *A Simple Probabilistic Model for Estimating the Risk of Standard Air Dives*. NEDU TR 04-42, Navy Experimental Diving Unit, Dec 2004.
14. H. D. Van Liew and E. T. Flynn, "Direct Ascent from Air and N₂-O₂ Saturation Dives in Humans: DCS Risk and Evidence of a Threshold," *Undersea Hyperbaric Medicine*, In Press.
15. S. S. Survanshi, E. D. Parker, E. D. Thalmann, and P. K. Weathersby, *Statistically Based Decompression Tables XII: Repetitive Decompression Tables for Air and Constant 0.7 ATA PO₂ in N₂ Using a Probabilistic Model*, Naval Medical Research Institute Technical Report 97-36, Naval Medical Research Institute, Aug 1997.
16. G. J. Duffner and H. H. Snider, "Effects of Exposing Men to Compressed Air and Helium-Oxygen Mixtures for 12 Hours at Pressures of 2–2.6 Atmospheres," NEDU Research Report 1-59, Navy Experimental Diving Unit, Jan 1959.
17. L. Wilkinson, *SYSTAT: The System for Statistics* (Evanston, IL: SYSTAT Inc., 1990).
18. H. V. Hempleman, "History of Decompression Procedures," in P. B. Bennett and D. H. Elliott, eds., *The Physiology and Medicine of Diving*, 4th ed. (Philadelphia, PA: Saunders, 1993), pp. 342–375.
19. J. Conkin, V. Kumar, M. P. Powell, P. P. Foster, and J. M. Waligora, "A Probabilistic Model of Hypobaric Decompression Sickness Based on 66 Chamber Tests," *Aviat Space Environ Med*, Vol. 67 (1996), pp. 176–183.
20. H. H. Ku, "Notes on the Use of Propagation of Error Formulas," *J Res Natl Bur Stand Eng Instr*, Vol. 70C (October-December 1966), pp. 263–273.
21. J. R. Hays, B. L. Hart, P. K. Weathersby, S. S. Survanshi, L. D. Homer, and E. T. Flynn, *Statistically Based Decompression Tables IV: Extension to Air and N₂O₂ Saturation Diving*, Naval Medical Research Institute Report 86-51, Naval Medical Research Institute, 1986.
22. P. K. Weathersby, S. S. Survanshi, and R. Y. Nishi, "Relative Decompression Risk of Dry and Wet Chamber Air Dives," *Undersea Biomed Res*, Vol. 17 (July 1990), pp. 333–352.

23. R. Ball, C. E. Lehner, and E. C. Parker, "Predicting Risk of Decompression Sickness in Humans from Outcomes in Sheep," *J Appl Physiol*, Vol. 86 (June 1999), pp. 1920–1929.
24. H. D. Van Liew and E. T. Flynn, "Use of Dive-Outcome Information Three Times in Preparation of a Probabilistic Decompression Model," *Undersea Hyperbaric Med*, Vol. 29 (Summer 2002), pp. 111–112.
25. E. D. Thalmann, *Suitability of the USN MK 15 (VVAL-18) Decompression Algorithm for Air Diving*, NEDU TR 03-12, Navy Experimental Diving Unit, Aug 2003 (originally published as Final Report on Research Contract N0463A-96-M-7036, March 30, 1997).
26. E. D. Thalmann, *Phase II Testing of Decompression Algorithms for Use in the U.S. Navy Underwater Decompression Computer*, NEDU Report 1-84, Navy Experimental Diving Unit, Jan 1984.
27. H. D. Van Liew and E. T. Flynn, "Probabilistic Models for Standard Air Dives: Effect of Inclusion of Saturation Data," *Undersea Hyperbaric Med*, Vol. 28 (Supplement 2001), p. 41.
28. C. D. Lehner and E. H. Lanphier, "Influence of Pressure Profile on DCS Symptoms," in R. D. Vann, ed., *The Physiological Basis of Decompression: 38th UHMS Workshop, Undersea and Hyperbaric Medical Society* (Bethesda, MD: UHMS, 1989), pp. 299–322.
29. C. D. Lehner, D. J. Hei, M. Palta, E. N. Lightfoot, and E. H. Lanphier, "Accelerated Onset of Decompression Sickness in Sheep after Short, Deep Dives," in A. A. Bove, A. J. Bachrach, and L. J. Greenbaum, eds., *9th International Symposium on Underwater and Hyperbaric Physiology* (Bethesda, MD: Undersea and Hyperbaric Medical Society, 1987), pp. 197–205.
30. R. D. Vann and E. D. Thalmann, "Decompression Physiology and Practice," in P. B. Bennett and D. H. Elliott, eds., *The Physiology and Medicine of Diving*, 4th ed. (Philadelphia, PA: Saunders, 1993), pp. 376–432.
31. E. T. Flynn, E. C. Parker, and R. Ball, "Risk of Decompression Sickness in Shallow No-Stop Air Diving: An Analysis of U.S. Navy Experience, 1990–1994," in N. E. Smith and M. R. Collie, eds., *Proceedings of the 14th Meeting of the United States–Japan Cooperative Program in Natural Resources (UJNR): Panel on Diving Physiology, Panama City, Florida, September 16–17, 1997* (Silver Spring, MD: U.S. Dept. of Commerce, NOAA, National Undersea Research Program, [1998]), pp. 23–38.

PAGE INTENTIONALLY LEFT BLANK

APPENDIX: DETAILS OF DCS CASES

DETAILS OF 104 DCS CASES IN THE NO-STOP SPREADSHEET (2,087 PERSON-DIVES)

Distilled from documentation of the U.S. Navy Decompression Database.⁴

Probability of DCS (P_{dcS}) is calculated according to the P-No-Stop Model

DCS type I or Type II, as commonly defined

DCS type II+ = a serious case of Type II DCS with major symptoms and usually fulminant onset

Rx = treatment in a recompression chamber: Y = yes, N = no

Case number	Source file	Profile number	Depth fswg	Bottom time, min	TDT, min	P_{dcS}	DCS type	Rx	Description
1	ASATARE	16	25.1	2,880	1.4	8.3%	I	Y	Bilateral knee pain
2	ASATARE	19	25.1	2,880	2.0	8.3%	I	Y	Right knee pain
3	ASATARE	27	25.1	2,880	3.0	8.3%	I	Y	Right knee pain
4	ASATARE	30	25.1	2,880	2.0	8.3%	I	Y	Left knee pain
5	ASATDC	4	26.4	1,440	1.0	7.7%	I	Y	Right knee, left ankle pain
6	ASATDC	6	33.0	1,440	1.0	28.9%	I	Y	Right knee, left ankle pain
7	ASATDC	7	33.0	1,440	1.0	28.9%	I	Y	Right knee pain, rash, mild nausea, malaise
8	ASATDC	9	33.0	1,440	1.0	28.9%	II+	Y	Marked right knee extensor weakness
9	ASATDC	10	33.0	1,440	1.0	28.9%	I	Y	Left shoulder pain
10	ASATDC	11	33.0	1,440	1.0	28.9%	I	Y	Right knee pain
11	ASATDC	13	26.4	1,440	1.0	7.7%	II	Y	Ache, slight weakness left quadriceps
12	ASATDC	15	33.0	1,454	1.0	29.2%	II	Y	Left shoulder pain, paresthesia left 5th digit
13	ASATNSM	7	29.5	2,880	1.4	21.9%	I	Y	Mild knee pain
14	ASATNSM	8	29.5	2,880	1.4	21.9%	I	Y	Knee pain
15	ASATNSM	9	29.5	2,880	1.4	21.9%	I	Y	Knee pain
16	ASATNSM	10	29.5	2,880	1.4	21.9%	I	Y	Ankle pain
17	ASATNMR	34	24.0	4,320	0.4	6.6%	I	Y	Left knee pain
18	DC4W	124	198.0	9	3.3	0.8%	I	Y	Shoulder pain
19	DC4W	127	231.0	7	3.9	0.5%	II+	Y	Vertigo, difficult breathing, syncope
20	DC4W	128	231.0	7	3.9	0.5%	II	Y	Right shoulder pain, weakness
21	DC4D	191	146.0	16	2.5	1.5%	I	Y	Labeled Type I; no narrative
22	EDU1351NL	14	94.0	48	3.8	8.4%	II	Y	Paresthesia, moderate fatigue
23	EDU1351NL	23	114.0	34	4.6	8.1%	II	Y	Itch, chest pain deep inspiration

APPENDIX: DETAILS OF DCS CASES

APPENDIX: DETAILS OF DCS CASES

57	EDU849S2	11	37.0	720	1.5	19.4%	I	Y	Right knee pain
58	EDU849S2	21	40.0	720	1.6	30.5%	I	N	Mild bilateral knee pain
59	EDU849S2	22	40.0	720	1.6	30.5%	I	N	Mild left knee pain
60	EDU849S2	25	40.0	720	1.6	30.5%	I	N	Right knee pain
61	EDU849S2	26	40.0	720	1.6	30.5%	I	N	Right knee pain
62	EDU849S2	30	40.0	720	1.6	30.5%	II	Y	Left wrist pain, left hand cold, left 5th digit flexed
63	EDU849S2	31	40.0	720	1.6	30.5%	I	Y	Right knee pain
64	EDU849S2	32	40.0	720	1.6	30.5%	I	Y	Right knee pain
65	EDU849S2	33	40.0	720	1.6	30.5%	I	Y	Left knee, right elbow pain
66	EDU849S2	34	40.0	720	1.6	30.5%	I	Y	Pain flexor tendons left thigh
67	EDU849S2	35	40.0	720	1.6	30.5%	I	Y	Left knee pain
68	EDU885	75	100.0	32	3.7	3.2%	I	Y	Left hip, shoulder, right elbow pain
69	EDU885	77	100.0	30	4.0	2.6%	I	Y	Left shoulder pain
70	EDU885	78	100.0	30	4.0	2.6%	I	Y	Left thumb pain
71	EDU885	79	100.0	30	4.0	2.6%	I	Y	Left elbow pain
72	EDUAS45	13	33.0	2,160	2.0	37.8%	I	Y	Bilateral knee pain
73	EDUAS45	14	33.0	2,160	2.0	37.8%	I	Y	Bilateral knee pain
74	NMR8697	6	85.5	30	1.5	1.2%	I	Y	Left upper arm pain
75	NMR8697	58	107.0	30	2.4	3.6%	I	N	Fleeting joint pains, fatigue
76	NMR8697	65	111.4	30	2.5	4.5%	I	Y	Right hip pain
77	NMR8697	74	57.0	60	1.1	1.1%	II	Y	Left wrist pain, decreased pinprick left hand
78	NMR8697	76	57.0	60	1.1	1.1%	II	Y	Slight weakness right leg, crossed abductor
79	NMR8697	132	66.6	60	1.8	2.3%	I	Y	Right shoulder pain
80	NMR8697	143	73.1	60	1.9	3.8%	I	Y	Mild pain superior and lateral to left eye
81	NMR8697	162	40.5	240	0.7	2.8%	I	N	Bilateral shoulder pain for 1 hr
82	NMR8697	173	30.0	240	1.2	0.7%	I	N	Right shoulder pain, not reported until resolved
83	NMR8697	184	42.7	240	0.7	3.7%	II	Y	Left shoulder pain; slight weakness left wrist, elbow
84	NMR8697	193	36.1	240	0.6	1.6%	II+	Y	Left post flank pain, erythema, hypoesthesia
85	NMR9209	6	23.3	4,303	12.0	5.6%	I	Y	Right shoulder, wrist pain
86	NMR9209	7	23.3	4,303	12.0	5.6%	I	Y	Bilateral ankle, knee pain
87	NMR97NOD	5	40.0	199	2.0	1.8%	I	Y	Right elbow pain
88	NMR97NOD	6	40.0	199	2.0	1.8%	II+	Y	Decreased hearing, mental status, memory
89	NMR97NOD	9	41.2	199	2.0	2.1%	II	Y	Rash, scintillating scotomata left visual field

APPENDIX: DETAILS OF DCS CASES

90	NEDU CORR	none	38.0	1,440		57.5%	I	Y	Bilateral knee pain
91	NMRNSW	8	61.5	92	1.2	4.0%	I	Y	Left upper arm pain
92	NMRNSW	19	61.5	106	1.3	5.3%	II	Y	Numbness right upper arm, hand
93	NMRNSW	23	61.5	102	1.2	4.9%	I	Y	Right knee pain
94	NMRNSW	25	61.5	92	1.2	4.0%	I	Y	Right knee pain
95	NMRNSW	28	61.5	82	1.1	3.1%	II+	Y	Paresthesia left side of body, left leg weakness, abnormal gait, perioral numbness, lightheadedness
96	NMR6H	13	38.0	359	0.8	4.7%	I	Y	Left hip pain
97	NMR6H	16	40.0	360	0.9	6.3%	I	Y	Right shoulder pain
98	NMR6H	18	40.0	360	0.7	6.3%	I	Y	Pain right hand, triceps, trapezius
99	PASA	24	101.5	35	3.1	4.5%	I	Y	Left shoulder pain
100	RNPLX50	3	33.0	720	1.1	9.8%	I	Y	Rash, joint pain, no narrative available
101	RNPLX50	8	35.0	720	1.2	13.9%	I	Y	Severe bend, no narrative available
102	RNPLX50	12	37.0	720	1.2	19.4%	I	Y	Bend, no narrative available
103	RNPLX50	16	41.0	720	1.4	34.9%	I	Y	Severe bend, no narrative available
104	RNPLX50	16	41.0	720	1.4	34.9%	I	Y	Bend, no narrative available

* A letter from CAPT Gerald Duffner MC USN (ret) of 14 Aug 2001 indicates that the DCS cases were Type I, but this information is from memory only.